

Table 1
Comparison of Unit 1, 16 EFPY Projected ARTs With Existing P/T Curve
Assumptions (°F)

ART Location	16 EFPY	P/T Curve Basis
T/4	177.1	183.7
3T/4	119.5	151.4

WCAP-15958, Revision 0

**Analysis of Capsule V from Pacific Gas and Electric Company Diablo
Canyon Unit 1 Reactor Vessel Radiation Surveillance Program**

Westinghouse Non-Proprietary Class 3

WCAP-15958
Revision 0

January 2003

Analysis of Capsule V from Pacific Gas and Electric Company Diablo Canyon Unit 1 Reactor Vessel Radiation Surveillance Program



WCAP-15958, Revision 0

**Analysis of Capsule V from Pacific Gas and Electric
Company Diablo Canyon Unit 1 Reactor Vessel Radiation
Surveillance Program**

**A. R. Rawluszki
J. Conermann
R. J. Hagler**

January 2003

Approved: 
J.A. Gresham, Manager
Engineering & Materials Technology

Westinghouse Electric Company LLC
Energy Systems
P.O. Box 355
Pittsburgh, PA 15230-0355

©2003 Westinghouse Electric Company LLC
All Rights Reserved

TABLE OF CONTENTS

LIST OF TABLES.....	iv
LIST OF FIGURES.....	vi
PREFACE	viii
EXECUTIVE SUMMARY	ix
1 SUMMARY OF RESULTS.....	1-1
2 INTRODUCTION.....	2-1
3 BACKGROUND	3-1
4 DESCRIPTION OF PROGRAM	4-1
5 TESTING OF SPECIMENS FROM CAPSULE V.....	5-1
5.1 OVERVIEW.....	5-1
5.2 CHARPY V-NOTCH IMPACT TEST RESULTS	5-3
5.3 TENSILE TEST RESULTS	5-5
5.4 WEDGE OPENING LOADING TESTS	5-5
6 RADIATION ANALYSIS AND NEUTRON DOSIMETRY	6-1
6.1 INTRODUCTION	6-1
6.2 DISCRETE ORDINATES ANALYSIS.....	6-2
6.3 NEUTRON DOSIMETRY.....	6-5
6.4 CALCULATIONAL UNCERTAINTIES	6-6
7 SURVEILLANCE CAPSULE REMOVAL SCHEDULE.....	7-1
8 REFERENCES.....	8-1
APPENDIX A LOAD-TIME RECORDS FOR CHARPY SPECIMEN TESTS.....	A-0
APPENDIX B CHARPY V-NOTCH SHIFT RESULTS FOR EACH CAPSULE PREVIOUS FIT VS. SYMMETRIC HYPERBOLIC TANGENT CURVE-FITTING METHOD (CVGRAPGH, VERSION 4.1).....	B-0
APPENDIX C CHARPY V-NOTCH PLOTS FOR EACH CAPSULE USING SYMMETRIC HYPERBOLIC TANGENT CURVE-FITTING METHOD	C-0
APPENDIX D DIABLO CANYON UNIT 1 SURVEILLANCE PROGRAM CREDIBILITY ANALYSIS	D-0
APPENDIX E VALIDATION OF THE RADIATION TRANSPORT MODELS BASED ON NEUTRON DOSIMETRY MEASUREMENTS.....	E-0

LIST OF TABLES

Table 4-1	Heat Treatment History of the Diablo Canyon Unit 1 Reactor Vessel Surveillance Materials.....	4-3
Table 4-2	Heat Treatment History of the HSST 02 Correlation Monitor Plate Material.....	4-3
Table 4-3	Chemical Composition (wt %) of the Diablo Canyon Unit 1 Reactor Vessel Surveillance Materials (Unirradiated).....	4-4
Table 5-1	Charpy V-Notch Data for the Diablo Canyon Unit 1 Intermediate Shell Plate B4106-3 Irradiated to a Fluence of 1.37×10^{19} n/cm ² (E > 1.0 MeV) (Longitudinal Orientation)	5-6
Table 5-2	Charpy V-notch Data for the Diablo Canyon Unit 1 Surveillance Weld Material Irradiated to a Fluence of 1.37×10^{19} n/cm ² (E > 1.0 MeV).....	5-7
Table 5-3	Charpy V-notch Data for the Diablo Canyon Unit 1 Heat-Affected-Zone (HAZ) Material Irradiated to a Fluence of 1.37×10^{19} n/cm ² (E > 1.0 MeV)	5-8
Table 5-4	Charpy V-notch Data for the Diablo Canyon Unit 1 Correlation Monitor Material Irradiated to a Fluence of 1.37×10^{19} n/cm ² (E > 1.0 MeV).....	5-9
Table 5-5	Instrumented Charpy Impact Test Results for the Diablo Canyon Unit 1 Intermediate Shell Plate B4106-3 Irradiated to a Fluence of 1.37×10^{19} n/cm ² (E > 1.0 MeV) (Longitudinal Orientation)	5-10
Table 5-6	Instrumented Charpy Impact Test Results for the Diablo Canyon Unit 1 Surveillance Weld Metal Irradiated to a Fluence of 1.37×10^{19} n/cm ² (E > 1.0 MeV)	5-11
Table 5-7	Instrumented Charpy Impact Test Results for the Diablo Canyon Unit 1 Heat-Affected-Zone (HAZ) Irradiated to a Fluence of 1.37×10^{19} n/cm ² (E > 1.0 MeV).....	5-12
Table 5-8	Instrumented Charpy Impact Test Results for the Diablo Canyon Unit 1 Correlation Monitor Metal Irradiated to a Fluence of 1.37×10^{19} n/cm ² (E > 1.0 MeV).....	5-13
Table 5-9	Effect of Irradiation to 1.37×10^{19} n/cm ² (E > 1.0 MeV) on the Capsule V Notch Toughness Properties of the Diablo Canyon Unit 1 Reactor Vessel Surveillance Materials.....	5-14
Table 5-10	Comparison of the Diablo Canyon Unit 1 Surveillance Material 30 ft-lb Transition Temperature Shifts and Upper Shelf Energy Decreases with Regulatory Guide 1.99, Revision 2, Predictions.....	5-15
Table 5-11	Tensile Properties of the Diablo Canyon Unit 1 Capsule V Reactor Vessel Surveillance Materials Irradiated to 1.37×10^{19} n/cm ² (E > 1.0 MeV).....	5-16

LIST OF TABLES (Cont.)

Table 6-1	Calculated Neutron Exposure Rates and Integrated Exposures At The Surveillance Capsule Center.....	6-10
Table 6-2	Calculated Azimuthal Variation of Maximum Exposure Rates And Integrated Exposures at the Reactor Vessel Clad/Base Metal Interface	6-14
Table 6-3	Relative Radial Distribution Of Neutron Fluence ($E > 1.0$ MeV) Within The Reactor Vessel Wall	6-18
Table 6-4	Relative Radial Distribution of Iron Atom Displacements (dpa) Within The Reactor Vessel Wall	6-18
Table 6-5	Calculated Fast Neutron Exposure of Surveillance Capsules Withdrawn from Diablo Canyon Unit 1	6-19
Table 6-6	Calculated Surveillance Capsule Lead Factors.....	6-19
Table 7-1	Diablo Canyon Unit 1 Reactor Vessel Surveillance Capsule Withdrawal Schedule	7-1

LIST OF FIGURES

Figure 4-1	Arrangement of Surveillance Capsules in the Diablo Canyon Unit 1 Reactor Vessel....	4-6
Figure 4-2	Capsule V Diagram Showing the Location of Specimens, Thermal Monitors, and Dosimeters	4-7
Figure 5-1	Charpy V-Notch Impact Energy vs. Temperature for Diablo Canyon Unit 1 Reactor Vessel Intermediate Shell Plate B4106-3 (Longitudinal Orientation)	5-17
Figure 5-2	Charpy V-Notch Lateral Expansion vs. Temperature for Diablo Canyon Unit 1 Reactor Vessel Intermediate Shell Plate B4106-3 (Longitudinal Orientation)	5-18
Figure 5-3	Charpy V-Notch Percent Shear vs. Temperature for Diablo Canyon Unit 1 Reactor Vessel Intermediate Shell Plate B4106-3 (Longitudinal Orientation)	5-19
Figure 5-4	Charpy V-Notch Impact Energy vs. Temperature for Diablo Canyon Unit 1 Reactor Vessel Weld Metal.....	5-20
Figure 5-5	Charpy V-Notch Lateral Expansion vs. Temperature for Diablo Canyon Unit 1 Reactor Weld Metal.....	5-21
Figure 5-6	Charpy V-Notch Percent Shear vs. Temperature for Diablo Canyon Unit 1 Reactor Vessel Weld Metal.....	5-22
Figure 5-7	Charpy V-Notch Impact Energy vs. Temperature for Diablo Canyon Unit 1 Reactor Vessel Heat-Affected-Zone Material.....	5-23
Figure 5-8	Charpy V-Notch Lateral Expansion vs. Temperature for Diablo Canyon Unit 1 Reactor Vessel Heat-Affected-Zone Material	5-24
Figure 5-9	Charpy V-Notch Percent Shear vs. Temperature for Diablo Canyon Unit 1 Reactor Vessel Heat-Affected-Zone Material.....	5-25
Figure 5-10	Charpy V-Notch Impact Energy vs. Temperature for Diablo Canyon Unit 1 Reactor Vessel Correlation Monitor Material	5-26
Figure 5-11	Charpy V-Notch Lateral Expansion vs. Temperature for Diablo Canyon Unit 1 Reactor Vessel Correlation Monitor Material	5-27
Figure 5-12	Charpy V-Notch Percent Shear vs. Temperature for Diablo Canyon Unit 1 Reactor Vessel Correlation Monitor Material	5-28
Figure 5-13	Charpy Impact Specimen Fracture Surfaces for Diablo Canyon Unit 1 Reactor Vessel Intermediate Shell Plate B4106-3 (Longitudinal Orientation)	5-29

LIST OF FIGURES (Cont.)

Figure 5-14	Charpy Impact Specimen Fracture Surfaces for Diablo Canyon Unit 1 Reactor Vessel Weld Metal.....	5-30
Figure 5-15	Charpy Impact Specimen Fracture Surfaces for Diablo Canyon Unit 1 Reactor Vessel Heat-Affected-Zone Metal.....	5-31
Figure 5-16	Charpy Impact Specimen Fracture Surfaces for Diablo Canyon Unit 1 Reactor Vessel Correlation Monitor Material	5-32
Figure 5-17	Tensile Properties for Diablo Canyon Unit 1 Reactor Vessel Intermediate Shell Plate B4106-3 (Longitudinal Orientation)	5-33
Figure 5-18	Tensile Properties for Diablo Canyon Unit 1 Reactor Vessel Weld Metal	5-34
Figure 5-19	Fractured Tensile Specimens from Diablo Canyon Unit 1 Reactor Vessel Intermediate Shell Plate B4106-3 (Longitudinal Orientation).....	5-35
Figure 5-20	Fractured Tensile Specimens from Diablo Canyon Unit 1 Reactor Vessel Weld Metal.....	5-36
Figure 5-21	Engineering Stress-Strain Curves for Intermediate Shell Plate B4106-3 Tensile Specimens E8 and E9 (Longitudinal Orientation).....	5-37
Figure 5-22	Engineering Stress-Strain Curves for Weld Metal Tensile Specimens W3 and W4	5-38
Figure 6-1	Diablo Canyon Unit 1 r, θ Reactor Geometry at the Core Midplane.....	6-8
Figure 6-2	Diablo Canyon Unit 1 r,z Reactor Geometry	6-9

PREFACE

This report has been technically reviewed and verified by:

Reviewer:

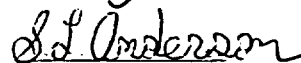
Sections 1 through 5, 7, 8, Appendices A, B, C and D

Section 6 and Appendix E

T. J. Laubham



S. L. Anderson



EXECUTIVE SUMMARY

The purpose of this report is to document the results of the testing of surveillance Capsule V from Diablo Canyon Unit 1. Capsule V was removed at 14.27 EFPY and post irradiation mechanical tests of the Charpy V-notch and tensile specimens were performed. A fluence evaluation utilizing the recently released neutron transport and dosimetry cross-section libraries was derived from the ENDF/B-VI database. Capsule V received a fluence of 1.37×10^{19} n/cm² after irradiation to 14.27 EFPY. This is equivalent to a vessel fluence at the end of the current license (32 EFPY). The peak clad/base metal interface vessel fluence after 14.27 EFPY of plant operation was 6.07×10^{18} n/cm². This evaluation lead to the following conclusions: Specimen results are behaving in accordance with predictions. The surveillance program, however, does not meet the regulatory criteria for credibility. Regulatory Guide 1.99 requires that all five criteria for credibility be met. For the Diablo Canyon Unit 1 surveillance program, four out of five of the criteria for credibility were met. A brief summary of the Charpy V-notch testing can be found in Section 1. All Charpy V-notch data was plotted using a symmetric hyperbolic tangent curve fitting program.

1 SUMMARY OF RESULTS

The analysis of the reactor vessel materials contained in surveillance Capsule V, the fifth capsule removed (third capsule tested) from the Diablo Canyon Unit 1 reactor pressure vessel, led to the following conclusions:

- The Charpy V-notch data presented in WCAP-8465^[3], WCAP-11567^[4] and WCAP-13750^[5] were based on Charpy curves using a hyperbolic tangent curve-fitting routine. The results presented in this report are based on a re-plot of all capsule data using CVGRAPH, Version 4.1, which is a symmetric hyperbolic tangent curve-fitting program. Appendix B presents a comparison of the Charpy V-Notch test results for each capsule based on previous fit vs. symmetric hyperbolic tangent fit. Appendix C presents the CVGRAPH, Version 4.1, Charpy V-notch plots and the program input data.
- Capsule V received an average fast neutron fluence ($E > 1.0$ MeV) of 1.37×10^{19} n/cm² after 14.27 effective full power years (EFPY) of plant operation.
- Irradiation of the reactor vessel intermediate shell plate B4106-3 (heat number C2793-1) Charpy specimens, oriented with the longitudinal axis of the specimen parallel to the major working direction (longitudinal orientation), resulted in an irradiated 30 ft-lb transition temperature of 39.46°F and an irradiated 50 ft-lb transition temperature of 77.51°F. This results in a 30 ft-lb transition temperature increase of 34.32°F and a 50 ft-lb transition temperature increase of 38.19°F for the longitudinal oriented specimens. See Table 5-9.
- Irradiation of the weld metal (heat number 27204) Charpy specimens resulted in an irradiated 30 ft-lb transition temperature of 135.45°F and an irradiated 50 ft-lb transition temperature of 219.26°F. This results in a 30 ft-lb transition temperature increase of 201.07°F and a 50 ft-lb transition temperature increase of 243.43°F. See Table 5-9.
- Irradiation of the weld Heat-Affected-Zone (HAZ) metal Charpy specimens resulted in an irradiated 30 ft-lb transition temperature of -52.65°F and an irradiated 50 ft-lb transition temperature of -1.98°F. This results in a 30 ft-lb transition temperature increase of 110.9°F and a 50 ft-lb transition temperature increase of 109.77°F. See Table 5-9.
- Irradiation of the Correlation Monitor Material Plate HSST02 Charpy specimens resulted in an irradiated 30 ft-lb transition temperature of 163.05°F and an irradiated 50 ft-lb transition temperature of 197.42°F. This results in a 30 ft-lb transition temperature increase of 116.61°F and a 50 ft-lb transition temperature increase of 119.12°F. See Table 5-9.
- The average upper shelf energy of the intermediate shell plate B4106-3 (longitudinal orientation) resulted in no energy decrease after irradiation. This results in an irradiated average upper shelf energy of 118 ft-lb for the longitudinal oriented specimens. See Table 5-9.

- The average upper shelf energy of the weld metal Charpy specimens resulted in an average energy decrease of 25 ft-lb after irradiation. This results in an irradiated average upper shelf energy of 66 ft-lb for the weld metal specimens. See Table 5-9.
- The average upper shelf energy of the weld HAZ metal Charpy specimens resulted in an average energy decrease of 20 ft-lb after irradiation. This results in an irradiated average upper shelf energy of 116 ft-lb for the weld HAZ metal. See Table 5-9.
- The average upper shelf energy of the Correlation Monitor Material Plate HSST02 Charpy specimens resulted in an average energy decrease of 6 ft-lb after irradiation. This results in an irradiated average upper shelf energy of 117 ft-lb for the weld correlation monitor metal. See Table 5-9.
- A comparison, as presented in Table 5-10, of the Diablo Canyon Unit 1 reactor vessel surveillance material test results with the Regulatory Guide 1.99, Revision 2^[1] predictions led to the following conclusions:
 - The measured 30 ft-lb shift in transition temperature for all the surveillance materials of Capsule V contained in the Diablo Canyon Unit 1 surveillance program are in good agreement or less than the Regulatory Guide 1.99, Revision 2, predictions.
 - The measured percent decrease in upper shelf energy for all the surveillance materials of Capsules V contained in the Diablo Canyon Unit 1 surveillance program are less than the Regulatory Guide 1.99, Revision 2 predictions.
- The credibility evaluation of the Diablo Canyon Unit 1 surveillance program presented in Appendix D of this report indicates that the surveillance results are not credible. This is based on not satisfying the third criterion for credibility.
- All beltline materials exhibit a more than adequate upper shelf energy level for continued safe plant operation and are predicted to maintain an upper shelf energy greater than 50 ft-lb throughout the life of the vessel (32 EFPY) as required by 10CFR50, Appendix G^[2].
- The calculated and best estimate end-of-license (32 EFPY) neutron fluence ($E > 1.0$ MeV) at the core midplane for the Diablo Canyon Unit 1 reactor vessel using the Regulatory Guide 1.99, Revision 2 attenuation formula (i.e., Equation #3 in the guide) are as follows:

Calculated:

- Vessel inner radius* = 1.26×10^{19} n/cm²
- Vessel 1/4 thickness = 7.51×10^{18} n/cm²
- Vessel 3/4 thickness = 2.67×10^{18} n/cm²

Best Estimate: Vessel inner radius* = 1.14×10^{19} n/cm²
Vessel 1/4 thickness = 6.79×10^{18} n/cm²
Vessel 3/4 thickness = 2.41×10^{18} n/cm²

*Clad/base metal interface

2 INTRODUCTION

This report presents the results of the examination of Capsule V, the third capsule removed and tested from the reactor in the continuing surveillance program which monitors the effects of neutron irradiation on the Pacific Gas and Electric Company Diablo Canyon Unit 1 reactor pressure vessel materials under actual operating conditions.

The surveillance program for the Pacific Gas and Electric Company Diablo Canyon Unit 1 reactor pressure vessel materials was designed and recommended by the Westinghouse Electric Corporation. A description of the surveillance program and the pre-irradiation mechanical properties of the reactor vessel materials are presented in WCAP-8465, "Pacific Gas and Electric Company Diablo Canyon Unit No. 1 Reactor Vessel Radiation Surveillance Program"^[3]. The original surveillance program was planned to cover the 40-year design life of the reactor pressure vessel and was based on ASTM E185-70, "Recommended Practice for Surveillance Tests for Nuclear Reactor Vessels." In 1992, Diablo Canyon implemented a Supplemental Surveillance Program^[25,26] to cover a 20 year extension on the current design life of the reactor vessel. The Supplemental Program was based on guidance from ASTM-E185-82, draft edition of ASTM-E185-92 and EPRI report, "Supplemental Reactor Vessel Surveillance Program Guidelines," dated December 1991. Capsule V was removed from the reactor after 14.27 EFPY of exposure and shipped to the Westinghouse Science and Technology Center Hot Cell Facility, where the post-irradiation mechanical testing of the Charpy V-notch impact and tensile surveillance specimens was performed.

The Charpy V-notch data presented in WCAP-8465^[3], WCAP-11567^[4] and WCAP-13750^[5] were based on a combination of hand-fit Charpy curves using engineering judgment and hyperbolic tangent curve-fitting. The only "hand fit" curves in the Diablo Canyon Unit 1 surveillance program were the unirradiated data curve fits done by W in WCAP-8465. The results presented in this report are based on a re-plot of all capsule data using CVGRAPH, Version 4.1, which is a symmetric hyperbolic tangent curve-fitting program. Appendix B presents a comparison of the Charpy V-Notch test results of previous curve fits vs. the symmetric hyperbolic tangent fit. Appendix C presents the CVGRAPH, Version 4.1, Charpy V-notch plots and the program input data.

3 BACKGROUND

The ability of the large steel pressure vessel containing the reactor core and its primary coolant to resist fracture constitutes an important factor in ensuring safety in the nuclear industry. The beltline region of the reactor pressure vessel is the most critical region of the vessel because it is subjected to significant fast neutron bombardment. The overall effects of fast neutron irradiation on the mechanical properties of low alloy, ferritic pressure vessel steels such as SA533 Grade B Class 1 (base material of the Diablo Canyon Unit 1 reactor pressure vessel beltline) are well documented in the literature. Generally, low alloy ferritic materials show an increase in hardness and tensile properties and a decrease in ductility and toughness during high-energy irradiation.

A method for ensuring the integrity of reactor pressure vessels has been presented in "Fracture Toughness Criteria for Protection Against Failure," Appendix G to Section XI of the ASME Boiler and Pressure Vessel Code^[16]. The method uses fracture mechanics concepts and is based on the reference nil-ductility transition temperature (RT_{NDT}).

RT_{NDT} is defined as the greater of either the drop weight nil-ductility transition temperature (NDTT per ASTM E-208^[15]) or the temperature 60°F less than the 50 ft-lb (and 35-mil lateral expansion) temperature as determined from Charpy specimens oriented perpendicular (transverse) to the major working direction of the plate. The RT_{NDT} of a given material is used to index that material to a reference stress intensity factor curve (K_{Ic} curve) which appears in Appendix G to the ASME Code^[16]. The K_{Ic} curve is a lower bound of static fracture toughness results obtained from several heats of pressure vessel steel. When a given material is indexed to the K_{Ic} curve, allowable stress intensity factors can be obtained for this material as a function of temperature. Allowable operating limits can then be determined using these allowable stress intensity factors.

RT_{NDT} and, in turn, the operating limits of nuclear power plants can be adjusted to account for the effects of radiation on the reactor vessel material properties. The changes in mechanical properties of a given reactor pressure vessel steel, due to irradiation, can be monitored by a reactor vessel surveillance program, such as the Diablo Canyon Unit 1 reactor vessel radiation surveillance program^[3], in which a surveillance capsule is periodically removed from the operating nuclear reactor and the encapsulated specimens tested. The increase in the average Charpy V-notch 30 ft-lb temperature (ΔRT_{NDT}) due to irradiation is added to the initial RT_{NDT} , along with a margin (M) to cover uncertainties, to adjust the RT_{NDT} (ART) for radiation embrittlement. This ART (RT_{NDT} initial + M + ΔRT_{NDT}) is used to index the material to the K_{Ic} curve and, in turn, to set operating limits for the nuclear power plant that take into account the effects of irradiation on the reactor vessel materials.

4 DESCRIPTION OF PROGRAM

Eight surveillance capsules for monitoring the effects of neutron exposure on the Diablo Canyon Unit 1 reactor pressure vessel core region (beltline) materials were inserted in the reactor vessel prior to initial plant start-up. The eight capsules were positioned in the reactor vessel between the thermal shield and the vessel wall as shown in Figure 4-1. The vertical center of the capsules is opposite the vertical center of the core. Three of the capsules contain specimens made from intermediate shell plate B4106-3, weld metal made with the same heat of weld wire (Heat No. 27204) as the limiting reactor vessel weld seam 3-442C and Correlation Monitor Plate HSST 02. The other five capsules contain specimens made from intermediate shell plates B4106-1, B4106-2, B4106-3 and Correlation Monitor Plate HSST 02.

Capsule V was removed after 14.27 effective full power years (EFPY) of plant operation. This capsule contained Charpy V-notch, tensile, and Wedge Opening Loading (WOL) specimens made from intermediate shell plate B4106-3 (heat number C2793-1) and submerged arc weld metal fabricated with the same weld wire heat 27204 and Linde 1092 flux type as used in the reactor vessel intermediate and lower shell longitudinal weld seams. In addition, this capsule contained Charpy V-notch specimens from the weld Heat-Affected-Zone (HAZ) metal of plate B4106-3 and SA533 Grade B Class 1 plate correlation monitor material.

Test material obtained from the Intermediate Shell Plate (after the thermal heat treatment and forming of the plate) was taken at least one plate thickness (9 5/8 inches) from the quenched edges of the plate. All test specimens were machined from the 1/4 thickness location of the plate after performing a simulated post-weld stress-relieving treatment. Specimens were machined from weld metal and heat-affected-zone metal from a stress-relieved weldment joining plates B4106-3 and B4106-1. All heat-affected-zone specimens were obtained from the weld heat-affected-zone of plate B4106-3.

Charpy V-notch impact specimens from intermediate shell plate B4106-3 were machined in the longitudinal orientation (longitudinal axis of the specimen parallel to the major rolling direction). The core region weld Charpy impact specimens were machined from the weldment such that the long dimension of each Charpy specimen was perpendicular to the weld direction. The notch of the weld metal Charpy specimens was machined such that the direction of crack propagation in the specimen was in the welding direction.

Tensile specimens from intermediate shell plate B4106-3 were machined in the longitudinal orientation. Tensile specimens from the weld metal were oriented with the long dimension of the specimen perpendicular to the weld direction.

WOL specimens from intermediate shell plate B4106-3 and weld metal were machined such that the simulated crack in the specimen would propagate normal and parallel to the major working direction for the plate specimen and parallel to the weld direction.

The heat treatment of the surveillance materials is presented in Tables 4-1 and 4-2. The chemical composition of the unirradiated surveillance material^[3] is presented in Table 4-3. No chemical analyses were performed for the surveillance materials in capsule V.

Capsule V contained dosimeter wires of pure copper, nickel, and aluminum 0.15 weight percent cobalt (cadmium-shielded and unshielded). In addition, cadmium shielded fission monitors of neptunium (Np^{237}) and uranium (U^{238}) were placed in the capsule to measure the integrated flux at specific neutron energy levels.

The capsule contained thermal monitors made from two low-melting-point eutectic alloys and sealed in Pyrex tubes. These thermal monitors were used to define the maximum temperature attained by the test specimens during irradiation. The composition of the two eutectic alloys and their melting points are as follows:

2.5% Ag, 97.5% Pb	Melting Point: 579°F (304°C)
1.75% Ag, 0.75% Sn, 97.5% Pb	Melting Point: 590°F (310°C)

The arrangement of the various mechanical specimens, dosimeters and thermal monitors contained in Capsule V is shown in Figure 4-2.

Material	Temperature (°F)	Time (hrs.)	Coolant
Intermediate Shell Plate B4106-3	1600 ± 50	4	Water Quench
	1225 ± 25	4	Air Cool
	1150 ± 25	40	Furnace Cool to 600°F
Weld Metal (heat # 27204)	1150 ± 25	40	Furnace Cool to 600°F

Notes:

- (a) This table was taken from WCAP-13750^[5].

Temperature (°F)	Time (hrs.)	Coolant
1675 ± 25	4	Air Cool
1600 ± 25	4	Water Quench
1225 ± 25	4	Furnace Cool
1150 ± 25	40	Furnace Cool to 600°F

Notes:

- (a) This table was taken from WCAP-13750^[5].

Table 4-3 Chemical Composition (wt%) of the Diablo Canyon Unit 1 Reactor Vessel Surveillance Materials (Unirradiated)^(c)

Element	Intermediate Shell Plate B4106-3	Weld Metal ^(b)	HSST 02	
			Ladle	Check
N	0.010	0.009	-	-
C	0.200	0.140	0.22	0.22
Si	0.250	0.450	0.22	0.25
Mo	0.460	0.480	0.53	0.52
Cu	0.077	0.210	-	0.14
Ni	0.460	0.980	0.62	0.68
Mn	1.330	1.360	1.45	1.48
Cr	0.035	0.060	-	-
V	0.001	0.001	-	-
Co	0.001 ^(a)	0.001 ^(a)	-	-
Sn	0.007	0.010	-	-
Zn	0.001 ^(a)	0.056	-	-
Ti	0.001 ^(a)	0.010	-	-
Zr	0.001 ^(a)	0.030	-	-
As	0.009	0.016	-	-
Sb	0.001	0.003	-	-
S	0.012	0.025	0.019	0.018
P	0.011	0.016	0.011	0.012
Al	0.036	0.018	-	-
B	0.003 ^(a)	0.03 ^(a)	-	-

Notes:

(a) Not detected, the number represents the minimum of detection.

(b) Surveillance weld was made of the same weld wire Heat 27204 and Linde 1092 Flux as the beltline region reactor vessel intermediate and lower shell longitudinal weld seams. Linde 1092 flux lot 3714 was used to fabricate the surveillance weld whereas flux lot 3724 and 3774 was used to fabricate the intermediate and lower shell longitudinal weld seams respectively.

(c) This table was taken from WCAP-13750^[5].

The best estimate copper and nickel weight percent remains as presented in the Diablo Canyon Unit 1 FSAR. The values used for the intermediate shell plate B4106-3 (Heat Number C2793-1) in all calculations documented in this report are as follows:

Cu wt. % = 0.086, and

Ni wt. % = 0.476

The values used for the surveillance weld (Heat Number 27204)* in all calculations documented in this report are as follows:

Cu wt. % = 0.198, and

Ni wt. % = 0.999

* The overall best estimate Cu and Ni for heat 27204 is 0.203 Cu and 1.018 Ni. These values are documented in the Diablo Canyon Unit 1 FSAR.

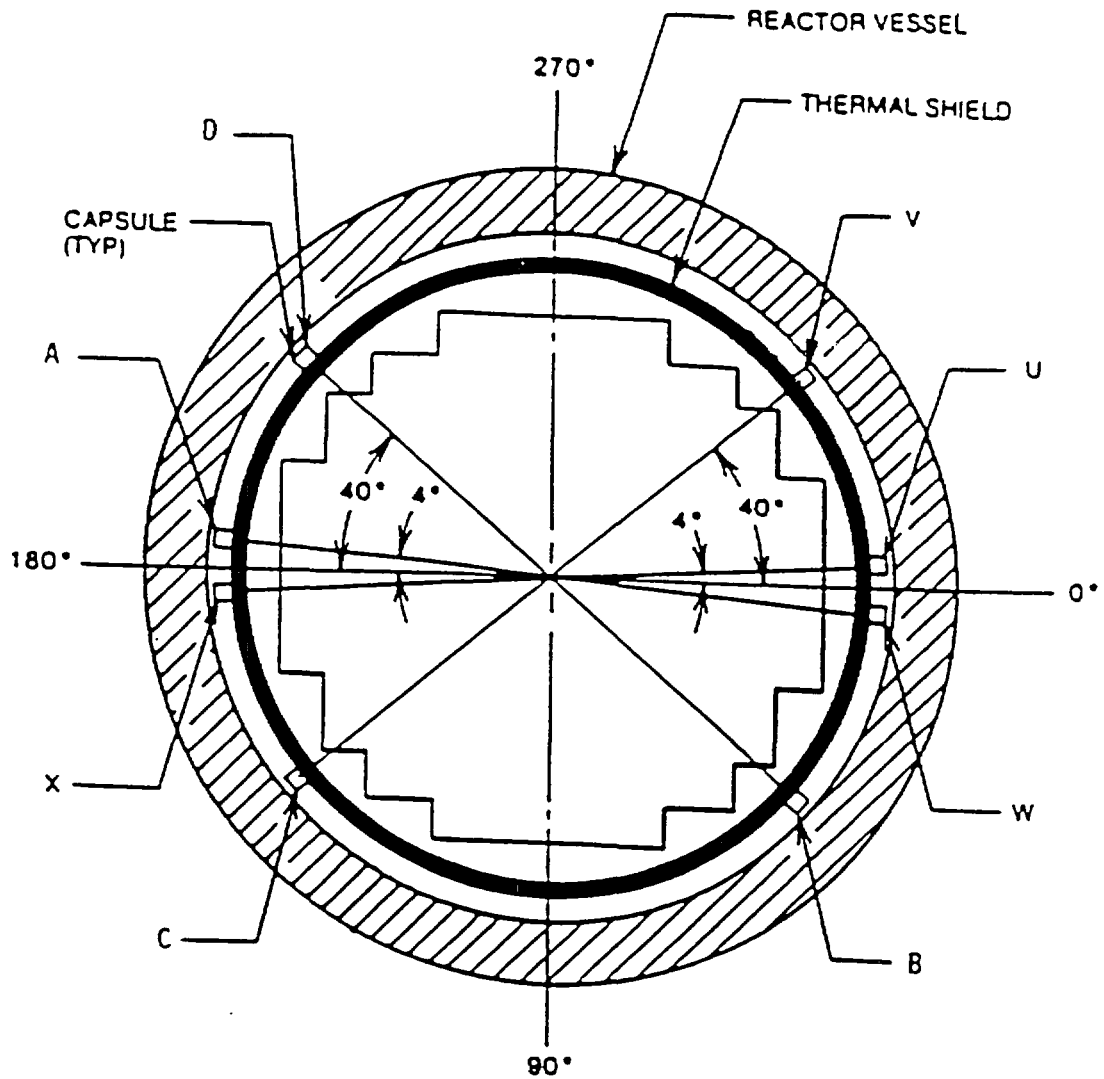


Figure 4-1 Arrangement of Surveillance Capsules in the Diablo Canyon Unit 1 Reactor Vessel

SPECIMEN NUMBERING CODE

E - PLATE B4106-3
 W - WELD METAL
 H - HEAT-AFFECTED ZONE
 R - CORRELATION MONITOR MATERIAL

SURVEILLANCE CAPSULE V

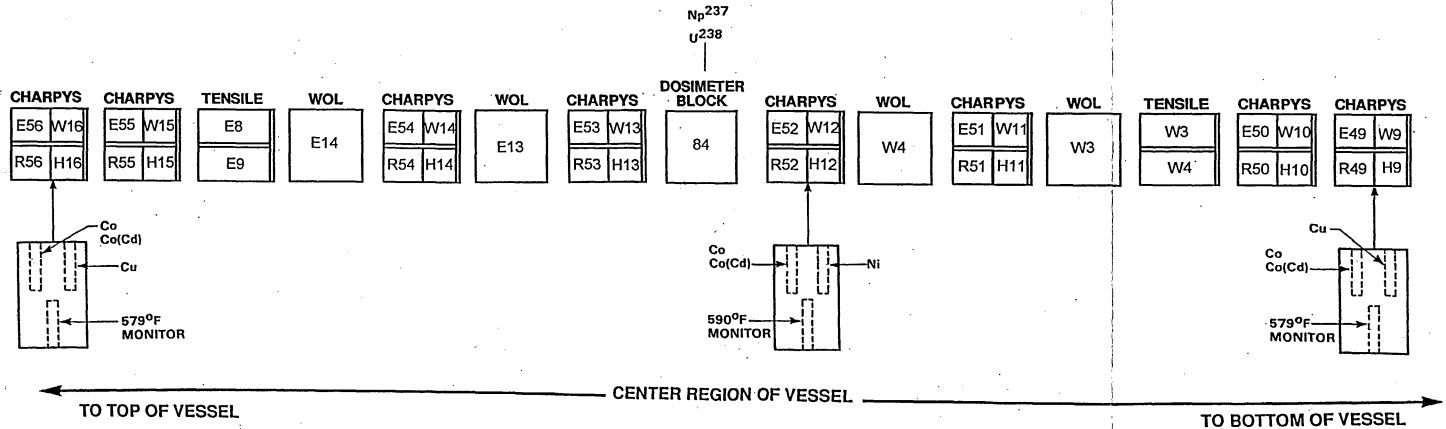


Figure 4-2 Capsule V Diagram Showing the Location of Specimens, Thermal Monitors, and Dosimeters

5 TESTING OF SPECIMENS FROM CAPSULE V

5.1 OVERVIEW

The post-irradiation mechanical testing of the Charpy V-notch impact specimens and tensile specimens was performed in the Remote Metallographic Facility (RMF) at the Westinghouse Science and Technology Center. Testing was performed in accordance with 10CFR50, Appendices G and H^[2], ASTM Specification E185-82^[6], and Westinghouse Procedure RMF 8402^[11], Revision 2 as modified by Westinghouse RMF Procedures 8102^[12], Revision 1, and 8103^[13], Revision 1.

Upon receipt of the capsule at the hot cell laboratory, the specimens and spacer blocks were carefully removed, inspected for identification number, and checked against the master list in WCAP-8465^[3]. No discrepancies were found.

Examination of the two low-melting point 579°F (304°C) and 590°F (310°C) eutectic alloys indicated no melting of either type of thermal monitor. Based on this examination, the maximum temperature to which the test specimens were exposed was less than 579°F (304°C).

The Charpy impact tests were performed per ASTM Specification E23-98^[7] and RMF Procedure 8103 on a Tinius-Olsen Model 74, 358J machine. The tup (striker) of the Charpy impact test machine is instrumented with an Instron Dynatup Impulse instrumentation system, feeding information into an IBM compatible computer. With this system, load-time and energy-time signals can be recorded in addition to the standard measurement of Charpy energy (E_D). From the load-time curve (Appendix A), the load of general yielding (P_{GY}), the time to general yielding (t_{GY}), the maximum load (P_M), and the time to maximum load (t_M) can be determined. Under some test conditions, a sharp drop in load indicative of fast fracture was observed. The load at which fast fracture was initiated is identified as the fast fracture load (P_F), and the load at which fast fracture terminated is identified as the arrest load (P_A).

The energy at maximum load (E_M) was determined by comparing the energy-time record and the load-time record. The energy at maximum load is approximately equivalent to the energy required to initiate a crack in the specimen. Therefore, the propagation energy for the crack (E_p) is the difference between the total energy to fracture (E_D) and the energy at maximum load (E_M).

The yield stress (σ_Y) was calculated from the three-point bend formula having the following expression:

$$\sigma_Y = (P_{GY} * L) / [B * (W - a)^2 * C] \quad (1)$$

where: L = distance between the specimen supports in the impact machine
 B = the width of the specimen measured parallel to the notch
 W = height of the specimen, measured perpendicularly to the notch
 a = notch depth

The constant C is dependent on the notch flank angle (ϕ), notch root radius (ρ) and the type of loading (i.e., pure bending or three-point bending). In three-point bending, for a Charpy specimen in which $\phi = 45^\circ$ and $\rho = 0.010$ inch, Equation 1 is valid with $C = 1.21$. Therefore, (for $L = 4W$),

$$\sigma_y = (P_{GY} * L) / [B * (W - a)^2 * 1.21] = (3.33 * P_{GY} * W) / [B * (W - a)^2] \quad (2)$$

For the Charpy specimen, $B = 0.394$ inch, $W = 0.394$ inch and $a = 0.079$ inch. Equation 2 then reduces to:

$$\sigma_y = 33.3 * P_{GY} \quad (3)$$

where σ_y is in units of psi and P_{GY} is in units of lbs. The flow stress was calculated from the average of the yield and maximum loads, also using the three-point bend formula.

The symbol A in columns 4, 5, and 6 of Tables 5-5 through 5-8 is the cross-section area under the notch of the Charpy specimens:

$$A = B * (W - a) = 0.1241 \text{ sq.in.} \quad (4)$$

Percent shear was determined from post-fracture photographs using the ratio-of-areas methods in compliance with ASTM Specification E23-98 and A370-97a^[8]. The lateral expansion was measured using a dial gage rig similar to that shown in the same specification.

Tensile tests were performed on a 20,000-pound Instron, split-console test machine (Model 1115) per ASTM Specification E8-99^[9] and E21-92 (1998)^[10], and Procedure RMF 8102. All pull rods, grips, and pins were made of Inconel 718. The upper pull rod was connected through a universal joint to improve axially of loading. The tests were conducted at a constant crosshead speed of 0.05 inches per minute throughout the test.

Extension measurements were made with a linear variable displacement transducer extensometer. The extensometer knife edges were spring-loaded to the specimen and operated through specimen failure. The extensometer gage length was 1.00 inch. The extensometer is rated as Class B-2 per ASTM E83-93^[18].

Elevated test temperatures were obtained with a three-zone electric resistance split-tube furnace with a 9-inch hot zone. All tests were conducted in air. Because of the difficulty in remotely attaching a thermocouple directly to the specimen, the following procedure was used to monitor specimen temperatures. Chromel-Alumel thermocouples were positioned at the center and at each end of the gage section of a dummy specimen and in each tensile machine gripper. In the test configuration, with a slight load on the specimen, a plot of specimen temperature versus upper and lower tensile machine gripper and controller temperatures was developed over the range from room temperature to 550°F. During the actual testing, the grip temperatures were used to obtain desired specimen temperatures. Experiments have indicated that this method is accurate to $\pm 2^\circ\text{F}$.

The yield load, ultimate load, fracture load, total elongation, and uniform elongation were determined directly from the load-extension curve. The yield strength, ultimate strength, and fracture strength were

calculated using the original cross-sectional area. The final diameter and final gage length were determined from post-fracture photographs. The fracture area used to calculate the fracture stress (true stress at fracture) and percent reduction in area was computed using the final diameter measurement.

5.2 CHARPY V-NOTCH IMPACT TEST RESULTS

The results of the Charpy V-notch impact tests performed on the various materials contained in Capsule V, which received a fluence of 1.37×10^{19} n/cm²(E > 1.0 MeV) in 14.27 EFPY of operation, are presented in Tables 5-1 through 5-8 and are compared with unirradiated results^[3] as shown in Figures 5-1 through 5-12.

The transition temperature increases and upper shelf energy decreases for the Capsule V materials are summarized in Table 5-9 and led to the following results:

Irradiation of the reactor vessel Intermediate Shell Plate B4106-3 (heat number C2793-1) Charpy specimens, oriented with the longitudinal axis of the specimen parallel to the major working direction (longitudinal orientation) resulted in an irradiated 30 ft-lb transition temperature of 39.46°F and an irradiated 50 ft-lb transition temperature of 77.51°F. This results in a 30 ft-lb transition temperature increase of 34.32°F and a 50 ft-lb transition temperature increase of 38.19°F for the longitudinal oriented specimens. See Table 5-9.

Irradiation of the weld metal (heat number 27204) Charpy specimens resulted in an irradiated 30 ft-lb transition temperature of 135.45°F and an irradiated 50 ft-lb transition temperature of 219.26°F. This results in a 30 ft-lb transition temperature increase of 201.07°F and a 50 ft-lb transition temperature increase of 243.43°F. See Table 5-9.

Irradiation of the weld Heat-Affected-Zone (HAZ) metal Charpy specimens resulted in an irradiated 30 ft-lb transition temperature of -52.65°F and an irradiated 50 ft-lb transition temperature of -1.98°F. This results in a 30 ft-lb transition temperature increase of 110.9°F and a 50 ft-lb transition temperature increase of 109.77°F. See Table 5-9.

Irradiation of the Correlation Monitor Material Plate HSST02 Charpy specimens resulted in an irradiated 30 ft-lb transition temperature of 163.05°F and an irradiated 50 ft-lb transition temperature of 197.42°F. This results in a 30 ft-lb transition temperature increase of 116.61°F and a 50 ft-lb transition temperature increase of 119.12°F. See Table 5-9.

The average upper shelf energy of the Intermediate Shell Plate B4106-3 (longitudinal orientation) resulted in no energy decrease after irradiation. This results in an irradiated average upper shelf energy of 118 ft-lb for the longitudinal oriented specimens. See Table 5-9.

The average upper shelf energy of the weld metal Charpy specimens resulted in an average energy decrease of 25 ft-lb after irradiation. This results in an irradiated average upper shelf energy of 66 ft-lb for the weld metal specimens. See Table 5-9.

The average upper shelf energy of the weld HAZ metal Charpy specimens resulted in an average energy decrease of 20 ft-lb after irradiation. This results in an irradiated average upper shelf energy of 116 ft-lb for the weld HAZ metal. See Table 5-9.

The average upper shelf energy of the weld correlation monitor metal Charpy specimens resulted in an average energy decrease of 6 ft-lb after irradiation. This results in an irradiated average upper shelf energy of 117 ft-lb for the weld correlation monitor metal. See Table 5-9.

A comparison, as presented in Table 5-10, of the Diablo Canyon Unit 1 reactor vessel beltline material test results with the Regulatory Guide 1.99, Revision 2^[1] predictions led to the following conclusions:

- The measured 30 ft-lb shift in transition temperature for all the surveillance materials of Capsule V contained in the Diablo Canyon Unit 1 surveillance program are in good agreement or less than the Regulatory Guide 1.99, Revision 2, predictions.
- The measured percent decrease in upper shelf energy for all the surveillance materials of Capsules V contained in the Diablo Canyon Unit 1 surveillance program are less than the Regulatory Guide 1.99, Revision 2 predictions.

The fracture appearance of each irradiated Charpy specimen from the various surveillance Capsule V materials is shown in Figures 5-13 through 5-16 and shows an increasingly ductile or tougher appearance with increasing test temperature.

All beltline materials exhibit a more than adequate upper shelf energy level for continued safe plant operation and are predicted to maintain an upper shelf energy greater than 50 ft-lb throughout the life of the vessel (32 EFPY) as required by 10CFR50, Appendix G^[2].

The load-time records for individual instrumented Charpy specimen tests are shown in Appendix A.

The Charpy V-notch data presented in WCAP-8465^[3], WCAP-11567^[4] and WCAP-13750^[5] were based on hyperbolic tangent curve fitting. The results presented in this report are based on a re-plot of all capsule data using CVGRAPH, Version 4.1^[14], which is a symmetric hyperbolic tangent curve-fitting program. Appendix B presents a comparison of the Charpy V-Notch test results for each capsule based on previous fit vs. symmetric hyperbolic tangent fit. Appendix C presents the CVGRAPH, Version 4.1, Charpy V-notch plots and the program input data.

5.3 TENSILE TEST RESULTS

The results of the tensile tests performed on the various materials contained in Capsule V irradiated to 1.37×10^{19} n/cm² (E> 1.0 MeV) are presented in Table 5-11 and are compared with unirradiated results^[3] as shown in Figures 5-17 and 5-18.

The results of the tensile tests performed on the Intermediate Shell Plate B4106-3 (longitudinal orientation) indicated that irradiation to 1.37×10^{19} n/cm² (E> 1.0 MeV) caused approximately a 7 to 12 ksi increase in the 0.2 percent offset yield strength and approximately a 5-11 ksi increase in the ultimate tensile strength when compared to unirradiated data^[3]. See Figure 5-17.

The results of the tensile tests performed on the surveillance weld metal indicated that irradiation to 1.37×10^{19} n/cm² (E> 1.0 MeV) caused approximately a 21 to 29 ksi increase in the 0.2 percent offset yield strength and approximately a 15 to 26 ksi increase in the ultimate tensile strength when compared to unirradiated data^[3]. See Figure 5-18.

The fractured tensile specimens for the Intermediate Shell Plate B4106-3 material are shown in Figure 5-19, while the fractured tensile specimens for the surveillance weld metal are shown in Figure 5-20. The engineering stress-strain curves for the tensile tests are shown in Figures 5-21 and 5-22.

5.4 WEDGE OPENING LOADING TESTS

Per the surveillance capsule testing contract, the Wedge Opening Loading (WOL) Specimens were not tested and are being stored at the Westinghouse Science and Technology Center Hot Cell facility.

Table 5-1 Charpy V-notch Data for the Diablo Canyon Unit 1 Intermediate Shell Plate B4106-3 Irradiated to a Fluence of 1.37×10^{19} n/cm² (E > 1.0 MeV) (Longitudinal Orientation)

Sample Number	Temperature		Impact Energy		Lateral Expansion		Shear %
	°F	°C	ft-lbs	Joules	mils	mm	
E52	-25	-32	15	20	5	0.13	5
E49	25	-4	32	43	19	0.48	10
E55	75	24	33	45	21	0.53	15
E51	110	43	70	95	46	1.17	45
E53	125	52	92	125	57	1.45	65
E50	175	79	94	127	56	1.42	75
E54	250	121	122	165	78	1.98	100
E56	275	135	119	161	80	2.03	100

Table 5-2 Charpy V-notch Data for the Diablo Canyon Unit 1 Surveillance Weld Metal Irradiated to a Fluence of 1.37×10^{19} n/cm² (E> 1.0 MeV)

Sample Number	Temperature		Impact Energy		Lateral Expansion		Shear %
	°F	°C	ft-lbs	Joules	mils	mm	
W11	25	-4	11	15	1	0.03	5
W13	100	38	23	31	13	0.33	15
W12	150	66	36	49	25	0.64	25
W9	200	93	37	50	24	0.61	30
W10	225	107	52	71	37	0.94	80
W15	300	149	71	96	51	1.30	100
W14	325	163	60	81	50	1.27	100
W16	350	177	66	89	48	1.22	100

**Table 5-3 Charpy V-notch Data for the Diablo Canyon Unit 1 Heat-Affected-Zone (HAZ)
Material Irradiated to a Fluence of 1.37×10^{19} n/cm² (E > 1.0 MeV)**

Sample Number	Temperature		Impact Energy		Lateral Expansion		Shear
	°F	°C	Ft-lbs	Joules	mils	mm	%
H14	-125	-87	19	26	4	0.10	10
H12	-50	-46	36	49	22	0.56	45
H11	0	-18	47	64	31	0.79	50
H10	72	22	66	89	45	1.14	75
H9	100	38	88	119	56	1.42	90
H15	125	52	128	174	71	1.80	100
H16	175	79	95	129	65	1.65	100
H13	225	107	124	168	79	2.01	100

Table 5-4 Charpy V-notch Data for the Diablo Canyon Unit 1 Correlation Monitor Material Irradiated to a Fluence of 1.37×10^{19} n/cm² (E > 1.0 MeV)

Sample Number	Temperature		Impact Energy		Lateral Expansion		Shear %
	°F	°C	Ft-lbs	Joules	mils	mm	
R49	25	-4	4	5	0	0.00	5
R51	50	10	8	11	3	0.08	10
R56	100	38	10	14	4	0.10	15
R55	150	66	33	45	20	0.51	30
R53	200	93	47	64	31	0.79	40
R54	250	121	74	100	48	1.22	65
R50	300	149	114	155	72	1.83	100
R52	325	163	120	163	80	2.03	100

**Table 5-5 Instrumented Charpy Impact Test Results for the Diablo Canyon Unit 1 Intermediate Shell Plate B4106-3
Irradiated to a Fluence of 1.37×10^{19} n/cm² (E>1.0 MeV) (Longitudinal Orientation)**

Sample No.	Test Temp. (°F)	Charpy Energy E _D (ft-lb)	Normalized Energies (ft-lb/in ²)			Yield Load P _{GY} (lb)	Time to Yield t _{GY} (msec)	Max. Load P _M (lb)	Time to Max. t _M (msec)	Fast Fract. Load P _F (lb)	Arrest Load P _A (lb)	Yield Stress S _Y (ksi)	Flow Stress (ksi)
			Charpy E _D /A	Max. E _M /A	Prop. E _P /A								
E52	-25	15	121	72	49	3939	0.19	4304	0.24	4289	0	131	137
E49	25	32	258	196	62	3323	0.14	4438	0.46	4409	0	111	129
E55	75	33	266	173	93	3222	0.15	4259	0.42	4251	702	107	125
E51	110	70	564	316	248	3241	0.15	4466	0.68	4237	751	108	128
E53	125	92	741	321	421	3306	0.16	4462	0.69	3569	1022	110	129
E50	175	94	757	296	461	2954	0.14	4288	0.67	3749	2058	98	121
E54	250	122	983	302	681	2957	0.15	4228	0.69	n/a	n/a	98	120
E56	275	119	959	290	669	3000	0.15	4182	0.67	n/a	n/a	100	120

Table 5-6 Instrumented Charpy Impact Test Results for the Diablo Canyon Unit 1 Surveillance Weld Metal Irradiated to a Fluence of 1.37×10^{19} n/cm² (E>1.0 MeV)

Sample No.	Test Temp. (°F)	Charpy Energy E _D (ft-lb)	Normalized Energies (ft-lb/in ²)			Yield Load P _{GY} (lb)	Time to Yield t _{GY} (msec)	Max. Load P _M (lb)	Time to Max. t _M (msec)	Fast Fract. Load P _F (lb)	Arrest Load P _A (lb)	Yield Stress S _Y (ksi)	Flow Stress (ksi)
			Charpy E _D /A	Max. E _M /A	Prop. E _P /A								
W11	25	11	89	47	42	3939	0.15	4227	0.18	4217	0	131	136
W13	100	23	185	74	112	3426	0.14	4473	0.23	4405	267	114	132
W12	150	36	290	202	89	3440	0.15	4431	0.46	4422	573	115	131
W9	200	37	298	198	100	3281	0.15	4395	0.46	4315	206	109	128
W10	225	52	419	202	217	3354	0.15	4443	0.46	4272	1309	112	130
W15	300	71	572	211	361	3276	0.15	4290	0.49	n/a	n/a	109	126
W14	325	60	483	191	293	3141	0.14	4051	0.47	n/a	n/a	105	120
W16	350	66	532	203	329	3138	0.15	4182	0.48	n/a	n/a	104	122

Table 5-7 Instrumented Charpy Impact Test Results for the Diablo Canyon Unit 1 Heat-Affected-Zone (HAZ) Metal Irradiated to a Fluence of 1.37×10^{19} n/cm² (E>1.0 MeV)

Sample No.	Test Temp. (°F)	Charpy Energy E _D (ft-lb)	Normalized Energies (ft-lb/in ²)			Yield Load P _{GY} (lb)	Time to Yield t _{GY} (msec)	Max. Load P _M (lb)	Time to Max. t _M (msec)	Fast Fract. Load P _F (lb)	Arrest Load P _A (lb)	Yield Stress S _Y (ksi)	Flow Stress (ksi)
			Charpy E _D /A	Max. E _M /A	Prop. E _P /A								
H14	-125	19	153	89	64	4907	0.19	5398	0.24	5388	0	163	172
H12	-50	36	290	79	212	3903	0.15	4927	0.23	4840	777.75	130	147
H11	0	47	379	80	299	4152	0.17	4822	0.24	4703	1027	138	149
H10	72	66	532	222	310	3733	0.15	4778	0.47	4099	2065	124	142
H9	100	88	709	248	461	3516	0.15	4700	0.53	3662	2376	117	137
H15	125	128	1031	247	785	3490	0.15	4676	0.53	n/a	n/a	116	136
H16	175	95	765	237	528	3406	0.15	4601	0.52	n/a	n/a	113	133
H13	225	124	999	236	763	3312	0.15	4505	0.53	n/a	n/a	110	130

Table 5-8 Instrumented Charpy Impact Test Results for the Diablo Canyon Unit 1 Correlation Monitor Metal Irradiated to a Fluence of 1.37×10^{19} n/cm² (E>1.0 MeV)

Sample No.	Test Temp. (°F)	Charpy Energy E _D (ft-lb)	Normalized Energies (ft-lb/in ²)			Yield Load P _{GY} (lb)	Time to Yield t _{GY} (msec)	Max. Load P _M (lb)	Time to Max. t _M (msec)	Fast Fract. Load P _F (lb)	Arrest Load P _A (lb)	Yield Stress S _Y (ksi)	Flow Stress (ksi)
			Charpy E _D /A	Max. E _M /A	Prop. E _P /A								
R49	25	4	32	14	18	1781	0.11	1839	0.12	1822	0	59	60
R51	50	8	64	36	29	3483	0.15	3593	0.16	3588	0	116	118
R56	100	10	81	36	44	3355	0.15	3465	0.17	3450	0	112	114
R55	150	33	266	185	81	3247	0.15	4399	0.44	4394	472	108	127
R53	200	47	379	229	150	3129	0.15	4449	0.53	4301	998	104	126
R54	250	74	596	301	295	3157	0.15	4377	0.67	4185	2576	105	125
R50	300	114	919	304	615	2971	0.15	4298	0.68	n/a	n/a	99	121
R52	325	120	967	313	654	3101	0.19	4228	0.73	n/a	n/a	103	122

Table 5-9 Effect of Irradiation to 1.37×10^{19} n/cm² (E>1.0 MeV) on the Capsule V Notch Toughness Properties of the Diablo Canyon Unit 1 Reactor Vessel Surveillance Materials^(c)												
Material	Average 30 (ft-lb)^(a) Transition Temperature (°F)			Average 35 mil Lateral^(b) Expansion Temperature (°F)			Average 50 ft-lb^(a) Transition Temperature (°F)			Average Energy Absorption^(a) at Full Shear (ft-lb)		
	Unirradiated	Irradiated	ΔT	Unirradiated	Irradiated	ΔT	Unirradiated	Irradiated	ΔT	Unirradiated	Irradiated	ΔE
Intermediate Shell Plate B4106-3 (Longitudinal)	5.14	39.46	34.32	28.65	89.72	61.07	39.31	77.51	38.19	118	121	3
Weld Metal (heat # 27204)	-65.62	135.45	201.07	-46.52	220.66	267.19	-24.16	219.26	243.43	91	66	-25
HAZ Metal	-163.55	-52.65	110.9	-107.5	18.76	126.27	-111.75	-1.98	109.77	136	116	-20
Correlation Monitor Material	46.44	163.05	116.61	58.96	213.46	154.49	78.3	197.42	119.12	123	117	-6

- a. "Average" is defined as the value read from the curve fit through the data points of the Charpy tests (see Figures 5-1, 5-4, 5-7 and 5-10).
- b. "Average" is defined as the value read from the curve fit through the data points of the Charpy tests (see Figures 5-2, 5-5, 5-8 and 5-11).
- c. Any difference in unirradiated properties reported in this Table in comparison to WCAP-8465, WCAP-11567 and WCAP-13750, are due to now using a symmetric hyperbolic tangent curve fitting of the Charpy data versus the method used in the previous analyses. See Appendix B.

Table 5-10 Comparison of the Diablo Canyon Unit 1 Surveillance Material 30 ft-lb Transition Temperature Shifts and Upper Shelf Energy Decreases with Regulatory Guide 1.99, Revision 2, Predictions

Material	Capsule	Fluence ^(d) ($\times 10^{19}$ n/cm ² , E > 1.0 MeV)	30 ft-lb Transition Temperature Shift		Upper Shelf Energy Decrease	
			Predicted (°F) ^(a)	Measured (°F) ^(b)	Predicted (%) ^(a)	Measured (%) ^(c)
Inter. Shell Plate B4106-3 (Longitudinal)	S	0.284	36.2	-1.78	14	0
	Y	1.05	56.0	48.66	19	6.8
	V	1.37	60.0	34.32	20	0
Weld Metal (heat # 27204)	S	0.284	145.8	110.79	25.5	11.0
	Y	1.05	225.4	232.59	34.5	34.1
	V	1.37	241.6	201.07	36.5	27.5
HAZ Metal	S	0.284	--	72.31	--	8.1
	Y	1.05	--	79.77	--	19.9
	V	1.37	--	110.9	--	14.7
Correlation Monitor Material	S	0.284	73.01	65.62	--	2.4
	Y	1.05	112.9	115.79	--	8.9
	V	1.37	121.0	116.61	--	4.9

Notes:

- (a) Based on Regulatory Guide 1.99, Revision 2, methodology using the mean weight percent values of copper and nickel of the surveillance material.
- (b) Calculated using measured Charpy data plotted using CVGRAPH, Version 4.1 (See Appendix C)
- (c) Values are based on the definition of upper shelf energy given in ASTM E185-82.
- (d) The fluence values presented here are the calculated fluence values, not the best estimate. For best estimate values see Section 6 of this report.

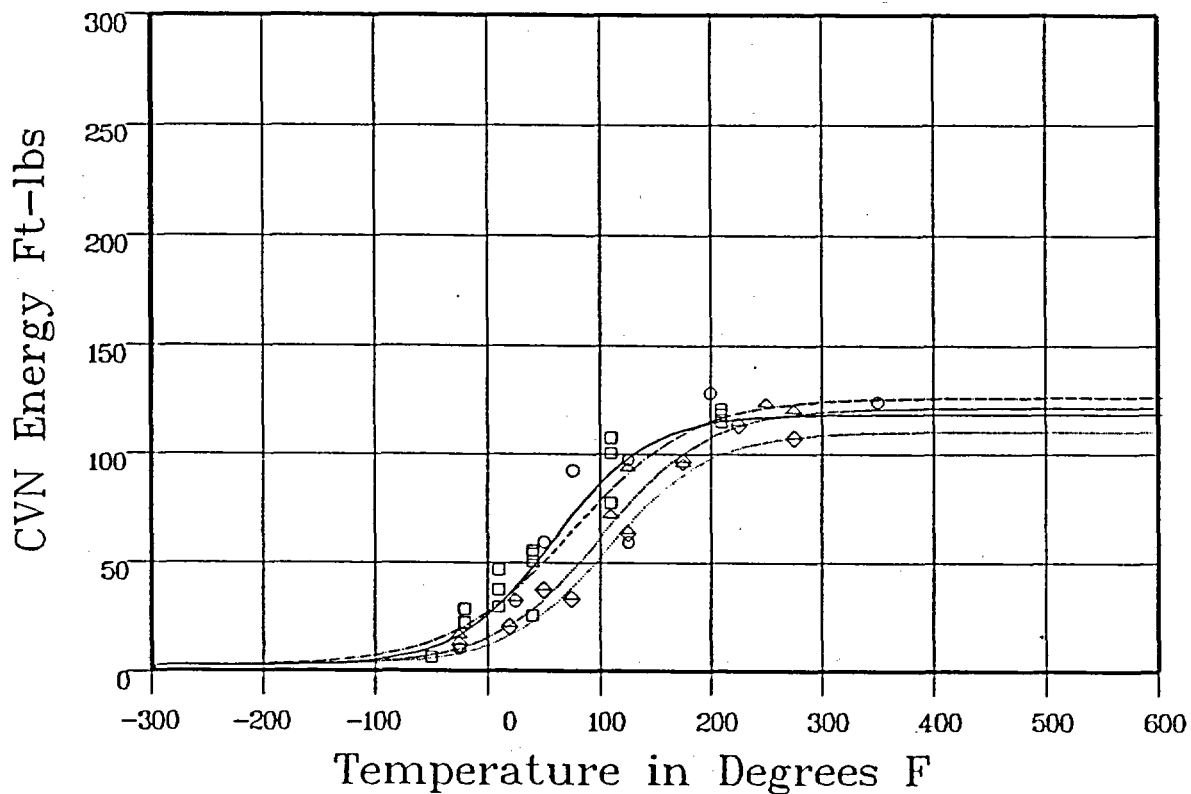
Table 5-11 Tensile Properties of the Diablo Canyon Unit 1 Capsule V Reactor Vessel Surveillance Materials Irradiated to 1.37×10^{19} n/cm² (E > 1.0 MeV)

Material	Sample Number	Test Temp. (°F)	0.2% Yield Strength (ksi)	Ultimate Strength (ksi)	Fracture Load (kip)	Fracture Stress (ksi)	Fracture Strength (ksi)	Uniform Elongation (%)	Total Elongation (%)	Reduction in Area (%)
Intermediate Shell Plate B4106-3 (Longitudinal)	E8	200	71.3	91.3	3.07	188.6	62.6	8.6	20.5	67
	E9	550	66.6	91.9	3.28	165.4	66.7	10.2	21.2	60
Weld Metal (heat # 27204)	W3	200	94.8	108.0	3.87	176.7	78.8	9.0	20.3	55
	W4	550	86.1	102.7	4.30	150.1	87.6	8.5	15.5	42

INTERMEDIATE SHELL PLATE B4106-3 (LONG)

CVGRAPH 4.1 Hyperbolic Tangent Curve Printed at 11:21:33 on 08-19-2002

Curve	Fluence	Results							
		LSE	d-LSE	USE	d-USE	T @ 30	d-T @ 30	T @ 50	d-T @ 50
1	0	2.19	0	118	0	5.14	0	39.31	0
2	2.84E+18	2.19	0	126	8	3.36	-1.78	45.43	6.11
3	1.05E+19	2.19	0	110	-8	53.81	48.66	91.82	52.51
4	1.37E+19	2.19	0	121	3	39.46	34.32	77.51	38.19



Curve Legend

1 \square ——— 2 \circ - - - - - 3 \diamond ——— 4 \triangle ———

Data Set(s) Plotted

Curve	Plant	Capsule	Material	Ori.	Heat#
1	DCI	UNIRR	PLATE SA533B1	LT	B4106-3
2	DCI	S	PLATE SA533B1	LT	B4106-3
3	DCI	Y	PLATE SA533B1	LT	B4106-3
4	DCI	V	PLATE SA533B1	LT	B4106-3

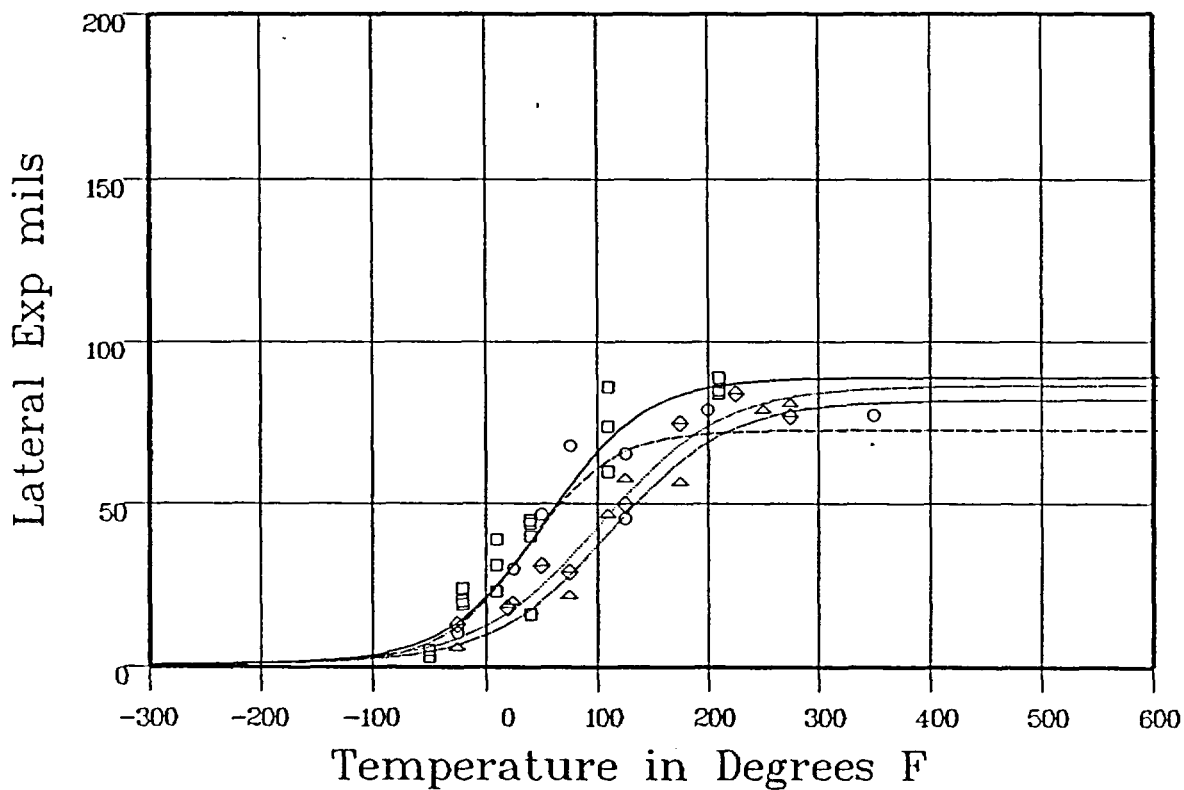
Figure 5-1 Charpy V-Notch Impact Energy vs. Temperature for Diablo Canyon Unit 1 Reactor Vessel Intermediate Shell Plate B4106-3 (Longitudinal Orientation)

INTERMEDIATE SHELL PLATE B4106-3 (LONG)

CVGRAPH 4.1 Hyperbolic Tangent Curve Printed at 11:38:29 on 08-19-2002

Results

Curve	Fluence	USE	d-USE	T \circ LE35	d-T \circ LE35
1	0	89.02	0	28.65	0
2	2.84E+18	72.72	-16.3	28.92	27
3	1.05E+19	86.52	-2.5	74.89	46.24
4	1.37E+19	81.97	-7.05	89.72	61.07



Curve Legend

1 \square ——— 2 \circ - - - - - 3 \diamond ——— 4 \triangle ———

Data Set(s) Plotted

Curve	Plant	Capsule	Material	Ori	Heat#
1	DCI	UNIRR	PLATE SA533B1	LT	B4106-3
2	DCI	S	PLATE SA533B1	LT	B4106-3
3	DCI	Y	PLATE SA533B1	LT	B4106-3
4	DCI	V	PLATE SA533B1	LT	B4106-3

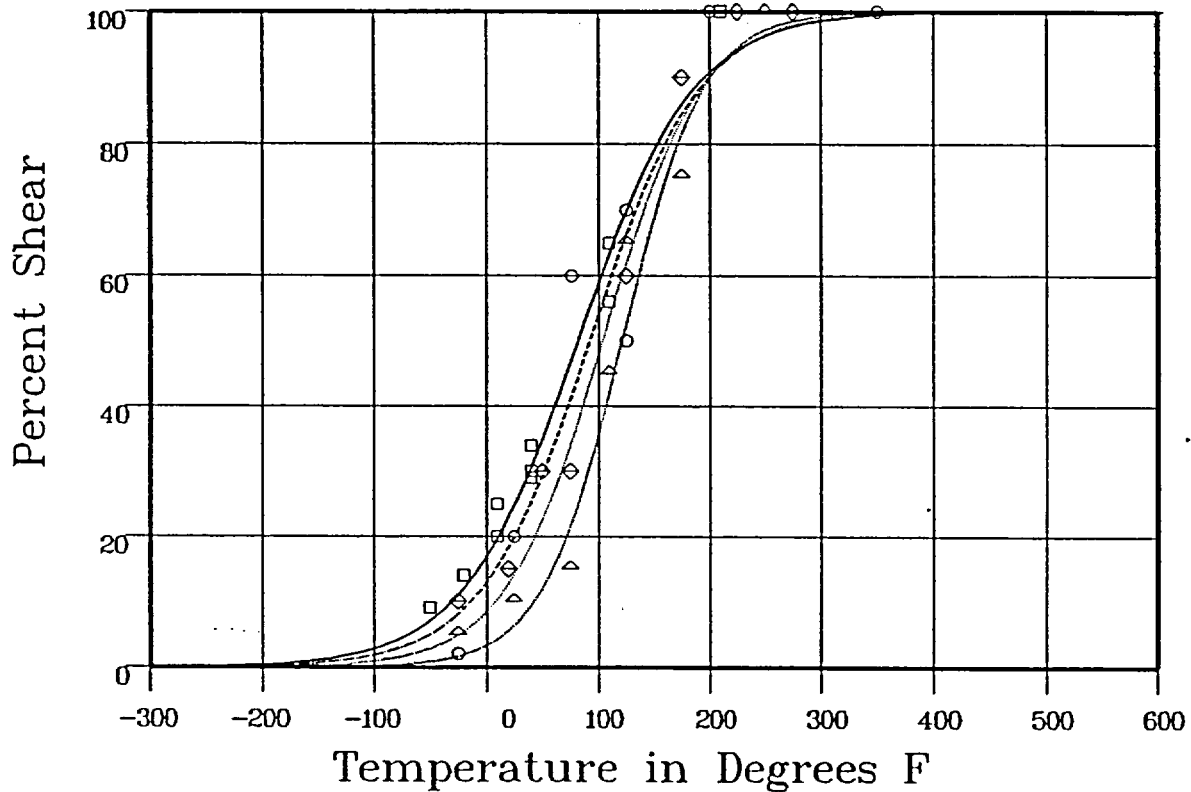
Figure 5-2 Charpy V-Notch Lateral Expansion vs. Temperature for Diablo Canyon Unit 1 Reactor Vessel Intermediate Shell Plate B4106-3 (Longitudinal Orientation)

INTERMEDIATE SHELL PLATE B4106-3

CVGRAPH 4.1 Hyperbolic Tangent Curve Printed at 11:49:00 on 08-19-2002

Results

Curve	Fluence	T @ 50% Shear	d-T @ 50% Shear
1	0	77.35	0
2	2.84E+18	87.89	10.53
3	1.05E+19	99.6	22.25
4	1.37E+19	117.18	39.83



Curve Legend

1 \square ——— 2 \circ - - - - 3 \diamond ——— 4 \triangle ———

Data Set(s) Plotted

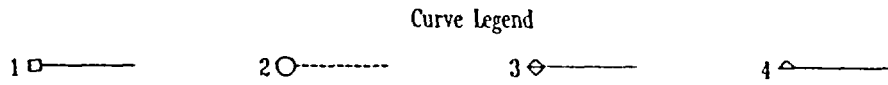
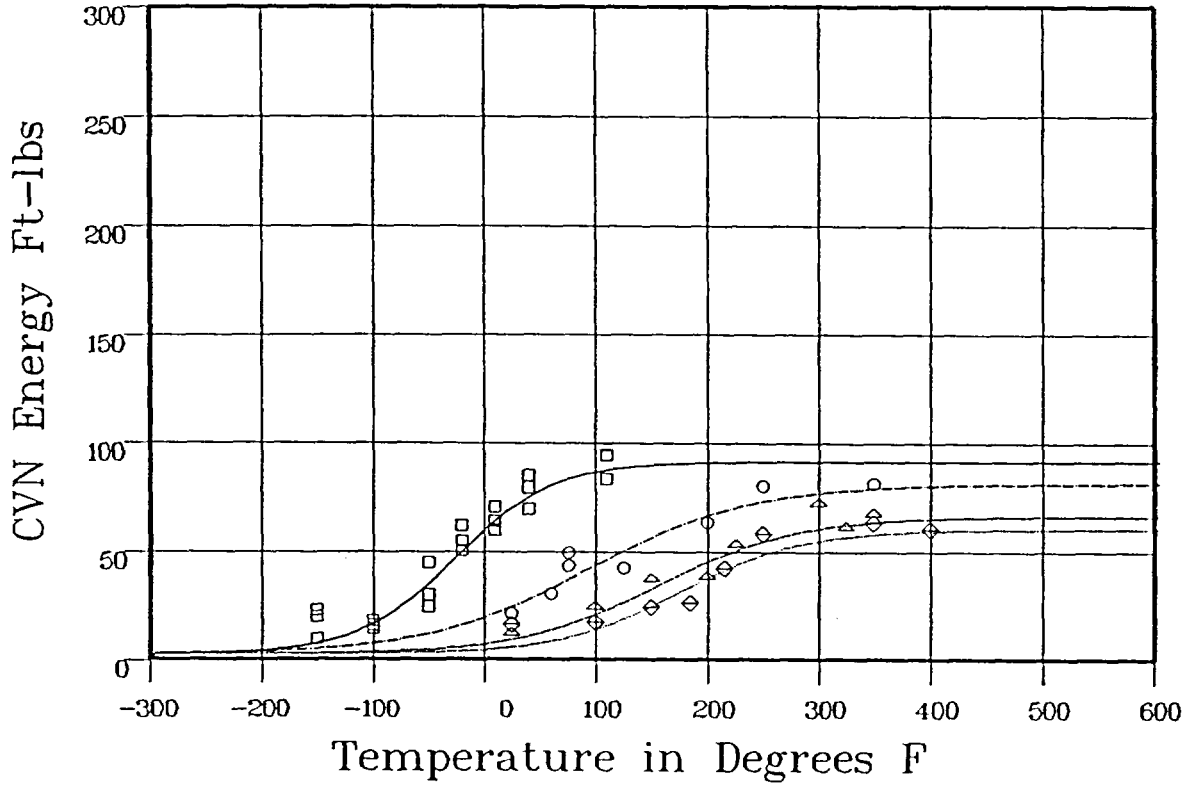
Curve	Plant	Capsule	Material	Ori.	Heat#
1	DCI	UNIRR	PLATE SA533B1	LT	B4106-3
2	DCI	S	PLATE SA533B1	LT	B4106-3
3	DCI	Y	PLATE SA533B1	LT	B4106-3
4	DCI	V	PLATE SA533B1	LT	B4106-3

Figure 5-3 Charpy V-Notch Percent Shear vs. Temperature for Diablo Canyon Unit 1 Reactor Vessel Intermediate Shell Plate B4106-3 (Longitudinal Orientation)

SURVEILLANCE WELD METAL

CVGRAPH 41 Hyperbolic Tangent Curve Printed at 1220:17 on 08-19-2002

Curve	Fluence	Results							
		LSE	d-LSE	USE	d-USE	T o 30	d-T o 30	T o 50	d-T o 50
1	0	2.19	0	91	0	-65.62	0	-24.16	0
2	2.84E+18	2.19	0	81	-10	45.17	110.79	120.38	144.54
3	1.05E+19	22	0	60	-31	166.97	232.59	255.73	279.9
4	1.37E+19	2.19	0	66	-25	135.45	201.07	219.26	243.43



Curve	Plant	Capsule	Data Set(s) Plotted			
			Material	Ori.	Heat#	
1	DCI	UNIRR	WELD LINDE 1092	27204	FLUX LOT 3714	
2	DCI	S	WELD LINDE 1092	27204	FLUX LOT 3714	
3	DCI	Y	WELD LINDE 1092	27204	FLUX LOT 3714	
4	DCI	V	WELD LINDE 1092	27204	FLUX LOT 3714	

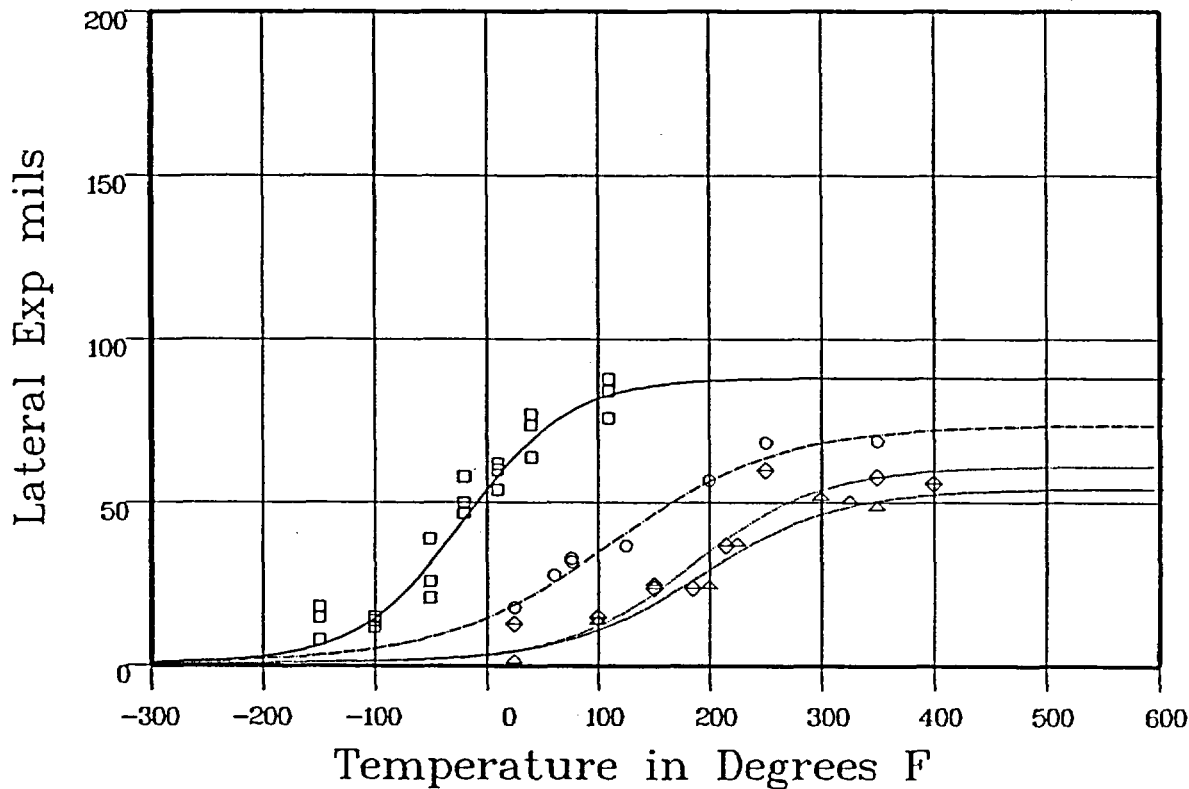
Figure 5-4 Charpy V-Notch Impact Energy vs. Temperature for Diablo Canyon Unit 1 Reactor Vessel Weld Metal

SURVEILLANCE PROGRAM WELD METAL

CVGRAPH 41 Hyperbolic Tangent Curve Printed at 1230:39 on 08-19-2002

Results

Curve	Fluence	USE	d-USE	T • LE35	d-T • LE35
1	0	88.17	0	-46.52	0
2	284E+18	73.91	-14.25	95.28	141.81
3	105E+19	61.24	-26.93	194.25	240.77
4	137E+19	54.47	-33.7	220.66	267.19



Curve Legend

1 □ ——— 2 ○ - - - - - 3 ◇ ——— 4 △ ———

Data Set(s) Plotted

Curve	Plant	Capsule	Material	Ori.	Heat#
1	DCI	UNIRR	WELD LINDE 1092	27204	FLUX LOT 3714
2	DCI	S	WELD LINDE 1092	27204	FLUX LOT 3714
3	DCI	Y	WELD LINDE 1092	27204	FLUX LOT 3714
4	DCI	Y	WELD LINDE 1092	27204	FLUX LOT 3714

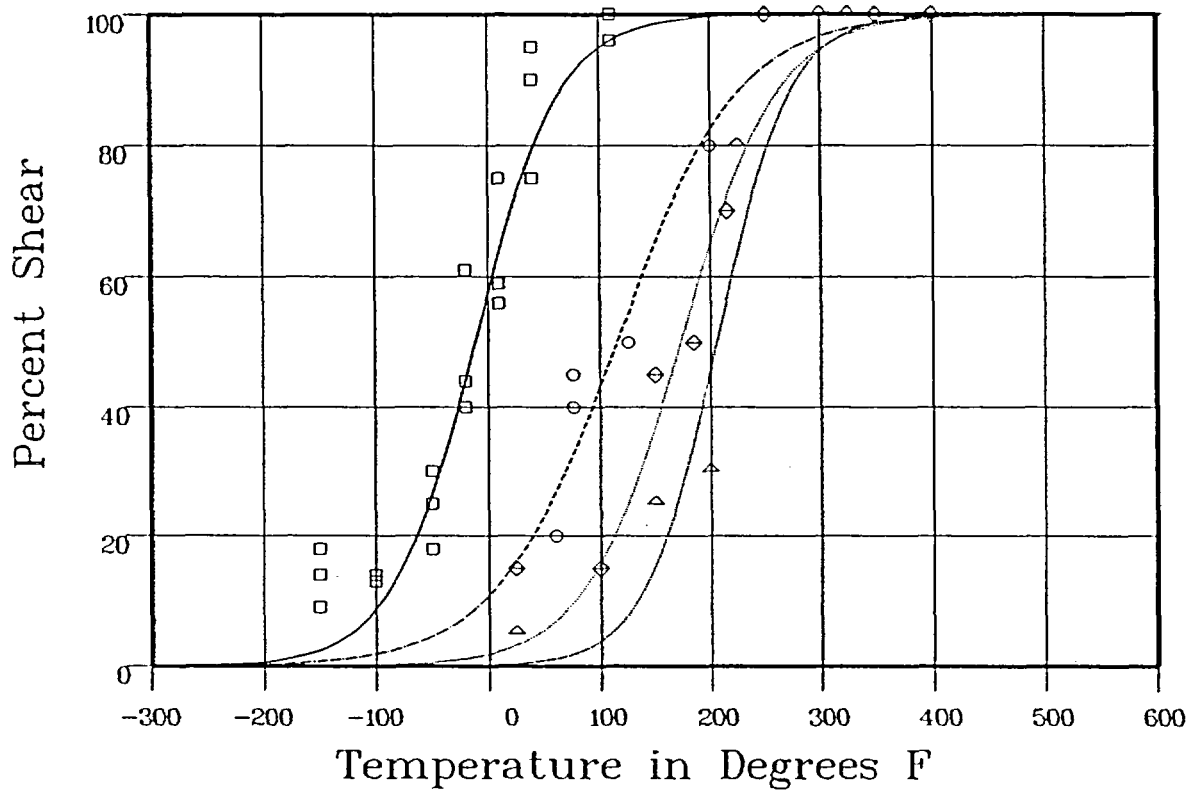
Figure 5-5 Charpy V-Notch Lateral Expansion vs. Temperature for Diablo Canyon Unit 1 Reactor Vessel Weld Metal

SURVEILLANCE PROGRAM WELD METAL

CVGRAPH 4.1 Hyperbolic Tangent Curve Printed at 124450 on 08-19-2002

Results

Curve	Fluence	T @ 50% Shear	d-T @ 50% Shear
1	0	-15.93	0
2	2.84E+18	110.74	126.67
3	1.05E+19	168.75	184.68
4	1.37E+19	201.56	217.5



Curve Legend

- 1 —
- 2 - - - -
- 3 —
- 4 —

Data Set(s) Plotted

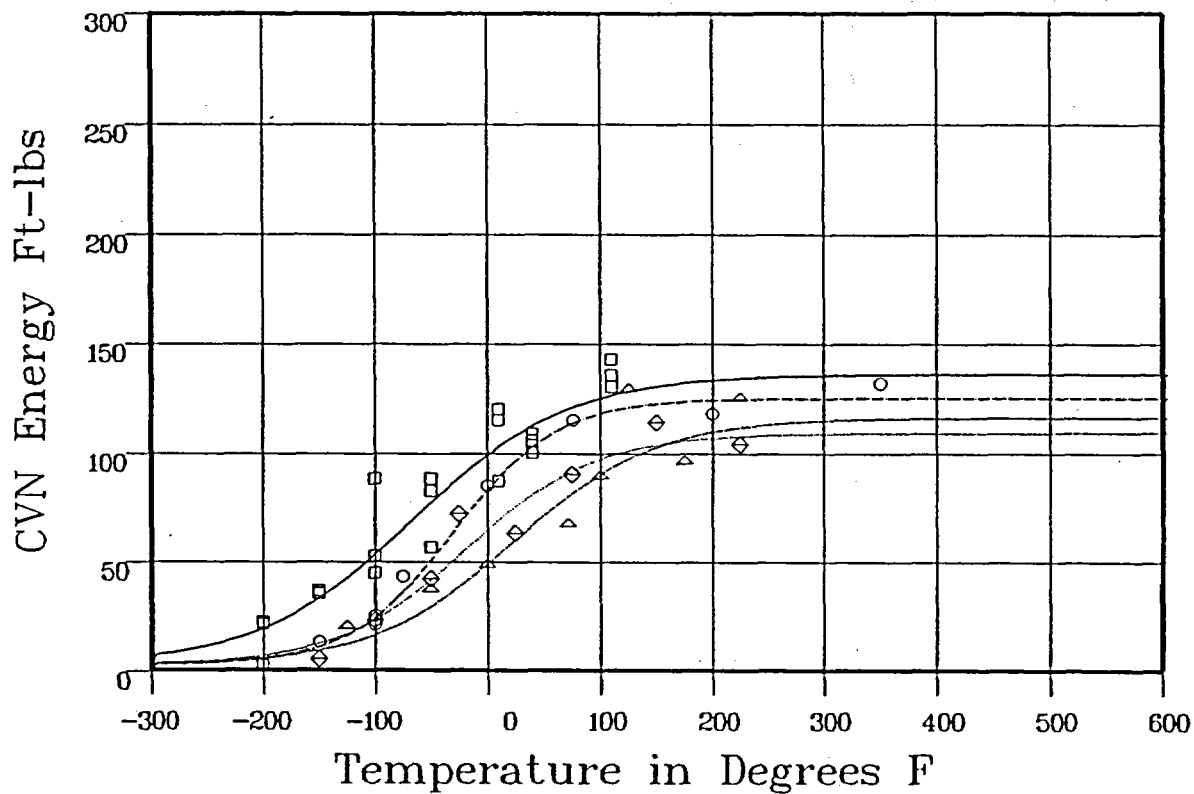
Curve	Plant	Capsule	Material	Ori.	Heat#
1	DCI	UNIRR	WELD LINDE 1092	27204	FLUX LOT 3714
2	DCI	S	WELD LINDE 1092	27204	FLUX LOT 3714
3	DCI	Y	WELD LINDE 1092	27204	FLUX LOT 3714
4	DCI	V	WELD LINDE 1092	27204	FLUX LOT 3714

Figure 5-6 Charpy V-Notch Percent Shear vs Temperature for Diablo Canyon Unit 1 Reactor Vessel Weld Metal

HEAT AFFECTED ZONE

CVGRAPH 4.1 Hyperbolic Tangent Curve Printed at 13:33:29 on 08-19-2002

Curve	Fluence	Results							
		LSE	d-LSE	USE	d-USE	T @ 30	d-T @ 30	T @ 50	d-T @ 50
1	0	2.19	0	136	0	-163.55	0	-111.75	0
2	2.84E+18	2.19	0	125	-11	-91.24	72.31	-55.29	56.46
3	1.05E+19	2.19	0	109	-27	-83.77	79.77	-35.96	75.78
4	1.37E+19	2.19	0	116	-20	-52.65	110.9	-1.98	109.77



Curve Legend

1 \square ——— 2 \circ - - - - - 3 \diamond ——— 4 \triangle ———

Data Set(s) Plotted

Curve	Plant	Capsule	Material	Ori.	Heat#
1	DC1	UNIRR	HEAT AFFD ZONE		
2	DC1	S	HEAT AFFD ZONE		
3	DC1	Y	HEAT AFFD ZONE		
4	DC1	V	HEAT AFFD ZONE		

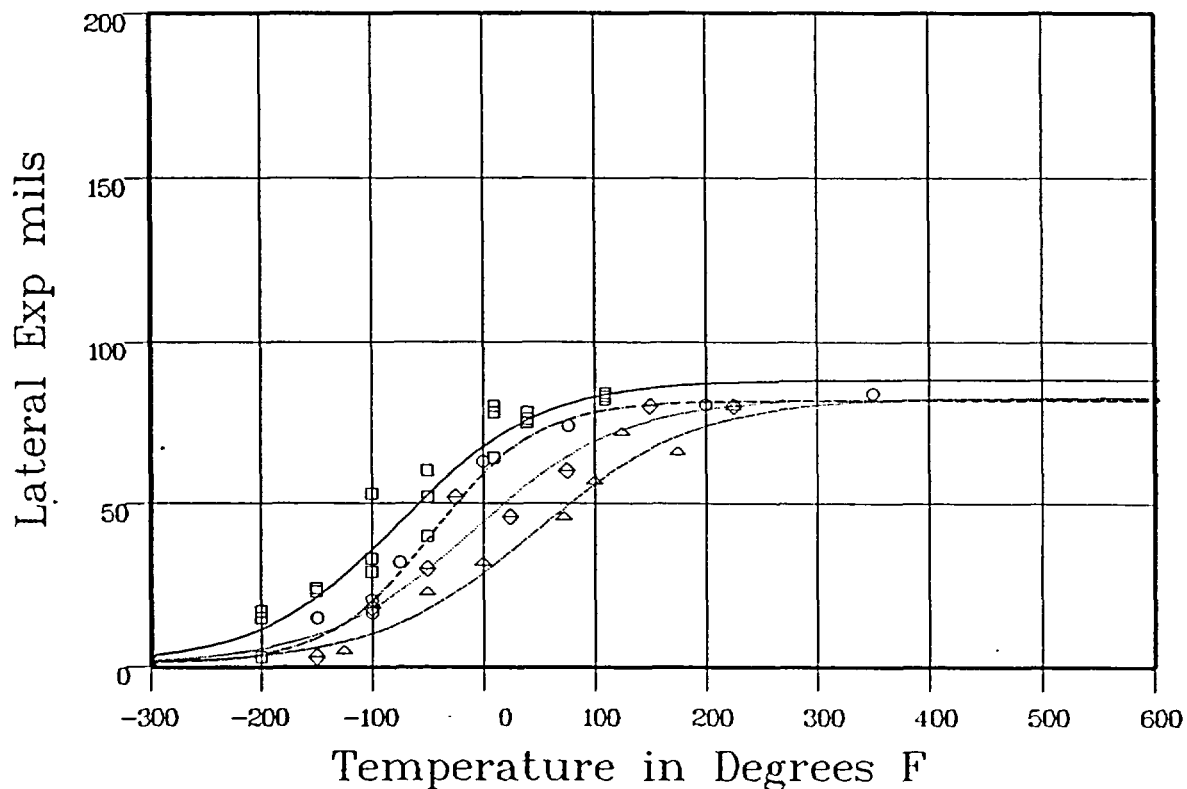
Figure 5-7 Charpy V-Notch Impact Energy vs. Temperature for Diablo Canyon Unit 1 Reactor Vessel Heat-Affected-Zone Material

HEAT AFFECTED ZONE

CVGRAPH 4.1 Hyperbolic Tangent Curve Printed at 14:27:03 on 08-19-2002

Results

Curve	Fluence	USE	d-USE	T σ LE35	d-T σ LE35
1	0	88.3	0	-107.5	0
2	2.84E+18	81.74	-6.56	-64.26	43.24
3	1.05E+19	82.45	-5.85	-36.47	71.03
4	1.37E+19	82.69	-5.61	18.76	126.27



Curve Legend

1 \square ——— 2 \circ - - - - - 3 \diamond ——— 4 \triangle ———

Data Set(s) Plotted

Curve	Plant	Capsule	Material	Ori.	Heat#
1	DCI	UNIRR	HEAT AFFD ZONE		
2	DCI	S	HEAT AFFD ZONE		
3	DCI	Y	HEAT AFFD ZONE		
4	DCI	V	HEAT AFFD ZONE		

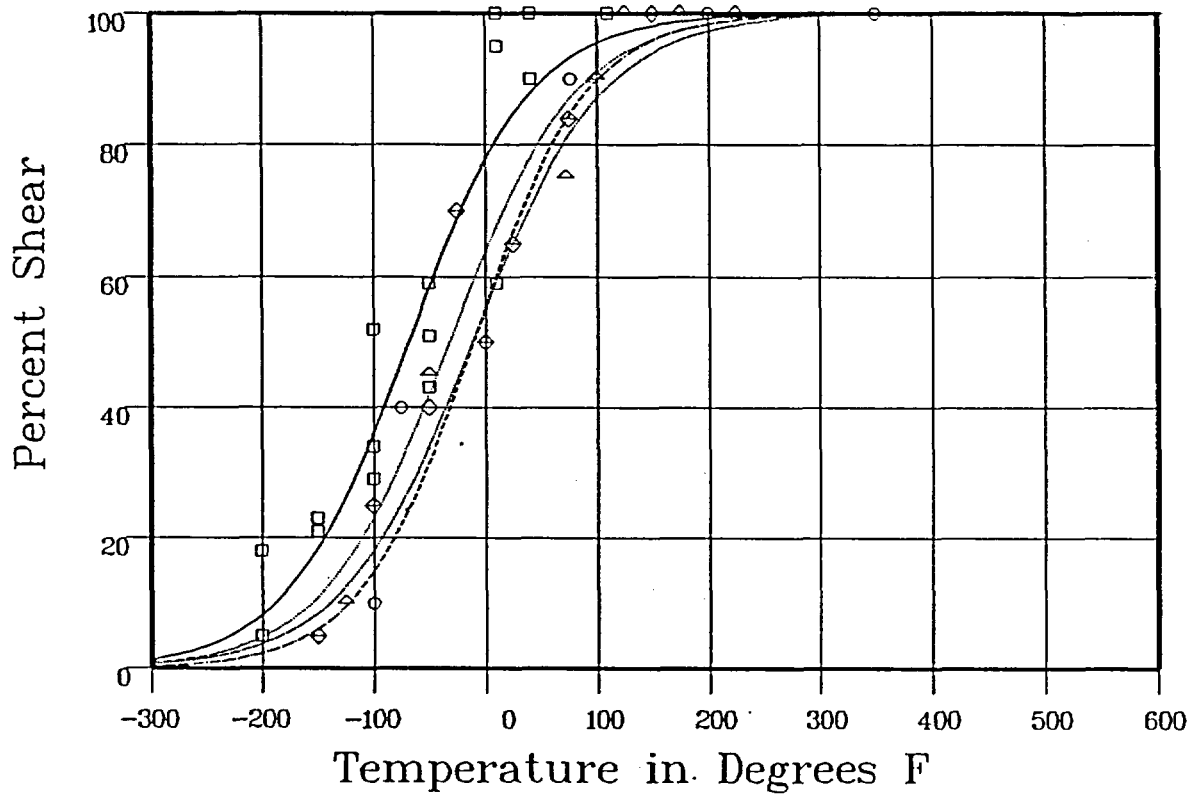
Figure 5-8 Charpy V-Notch Lateral Expansion vs. Temperature for Diablo Canyon Unit 1 Reactor Vessel Heat-Affected-Zone Material

HEAT AFFECTED ZONE

CVGRAPH 4.1 Hyperbolic Tangent Curve Printed at 14:01:24 on 09-03-2002

Results

Curve	Fluence	T @ 50% Shear	d-T @ 50% Shear
1	0	-72.94	0
2	2.84E+18	-15.46	57.47
3	1.05E+19	-36.27	36.66
4	1.37E+19	-15.93	57



Curve Legend



Data Set(s) Plotted

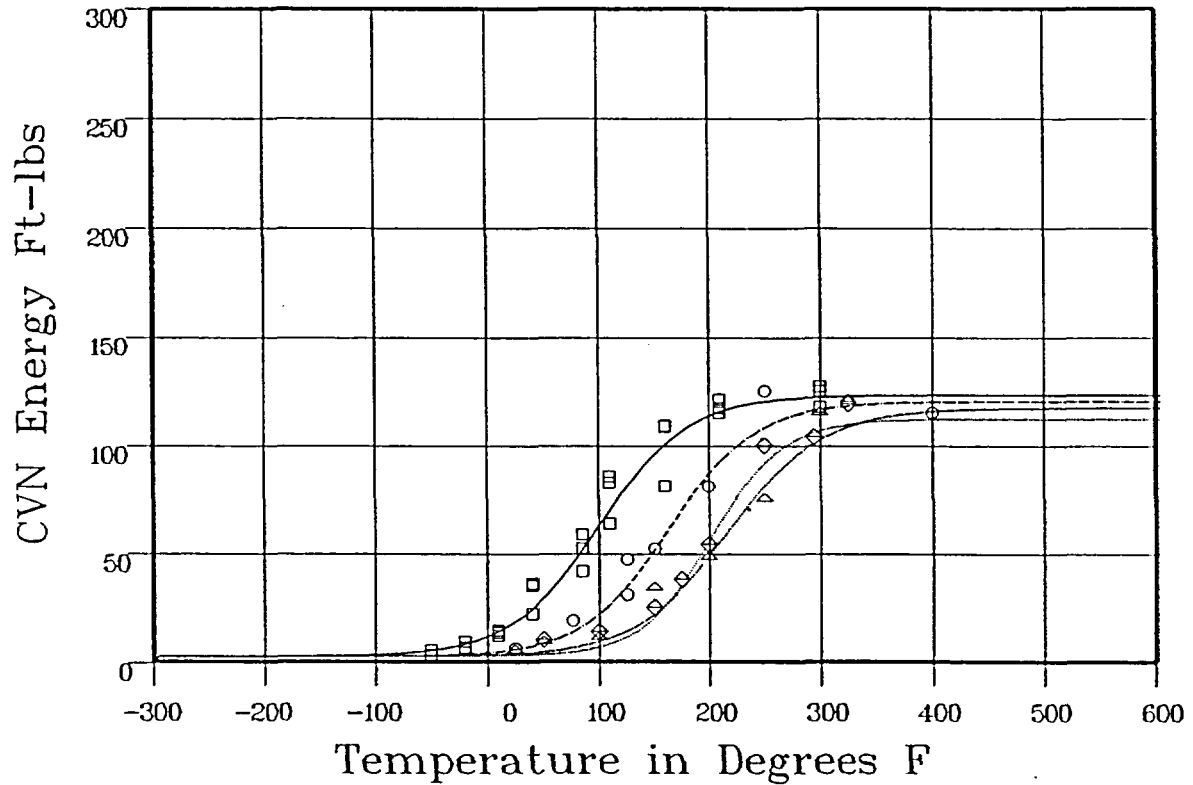
Curve	Plant	Capsule	Material	Ori.	Heat#
1	DCI	UNIRR	HEAT AFFD ZONE		
2	DCI	S	HEAT AFFD ZONE		
3	DCI	Y	HEAT AFFD ZONE		
4	DCI	V	HEAT AFFD ZONE		

Figure 5-9 Charpy V-Notch Percent Shear vs. Temperature for Diablo Canyon Unit 1 Reactor Vessel Heat-Affected-Zone Material

STANDARD REFERENCE MATERIAL

CVGRAPH 41 Hyperbolic Tangent Curve Printed at 11:05:06 on 09-06-2002

Curve	Fluence	Results							
		LSE	d-LSE	USE	d-USE	T o 30	d-T o 30	T o 50	d-T o 50
1	0	2.19	0	123	0	46.44	0	78.3	0
2	2.84E+18	2.19	0	120	-3	112.06	65.62	143.42	65.11
3	1.05E+19	2.19	0	112	-11	162.23	115.79	188.9	110.59
4	1.37E+19	2.19	0	117	-6	163.05	116.61	197.42	119.12



Curve Legend

1 □ ——— 2 ○ - - - - 3 ◇ ——— 4 △ ———

Data Set(s) Plotted

Curve	Plant	Capsule	Material	Ori.	Heat#
1	DCI	UNIRR	SRM SA533B1	LT	
2	DCI	S	SRM SA533B1	LT	
3	DCI	Y	SRM SA533B1	LT	
4	DCI	V	SRM SA533B1	LT	

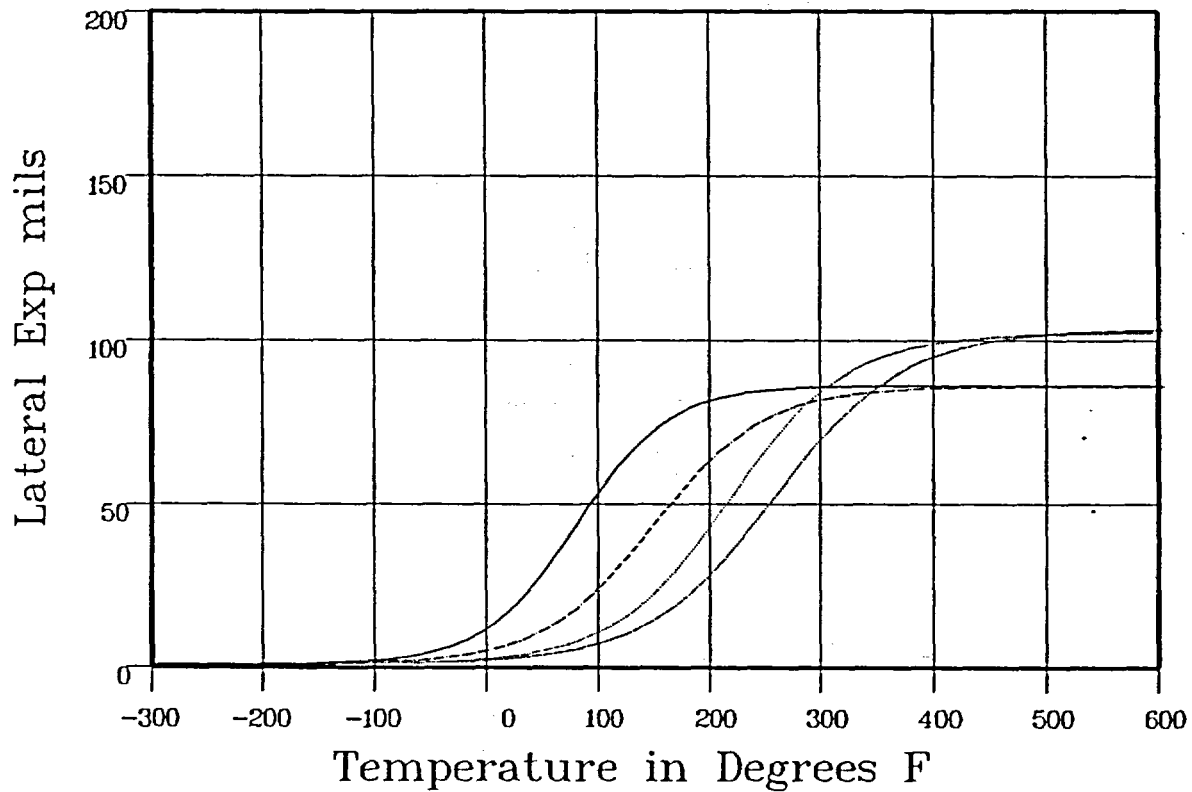
Figure 5-10 Charpy V-Notch Impact Energy vs. Temperature for Diablo Canyon Unit 1 Reactor Vessel Correlation Monitor Material

STANDARD REFERENCE MATERIAL

CVGRAPH 41 Hyperbolic Tangent Curve Printed at 11:09:33 on 09-06-2002

Results

Curve	Fluence	USE	d-USE	T σ LE35	d-T σ LE35
1	0	86.31	0	58.96	0
2	284E+18	85.97	-34	124.49	65.53
3	105E+19	102.39	16.07	178.01	119.05
4	137E+19	103.54	17.23	213.46	154.49



Curve Legend

1 \square ——— 2 \circ - - - - - 3 \diamond ——— 4 \triangle ———

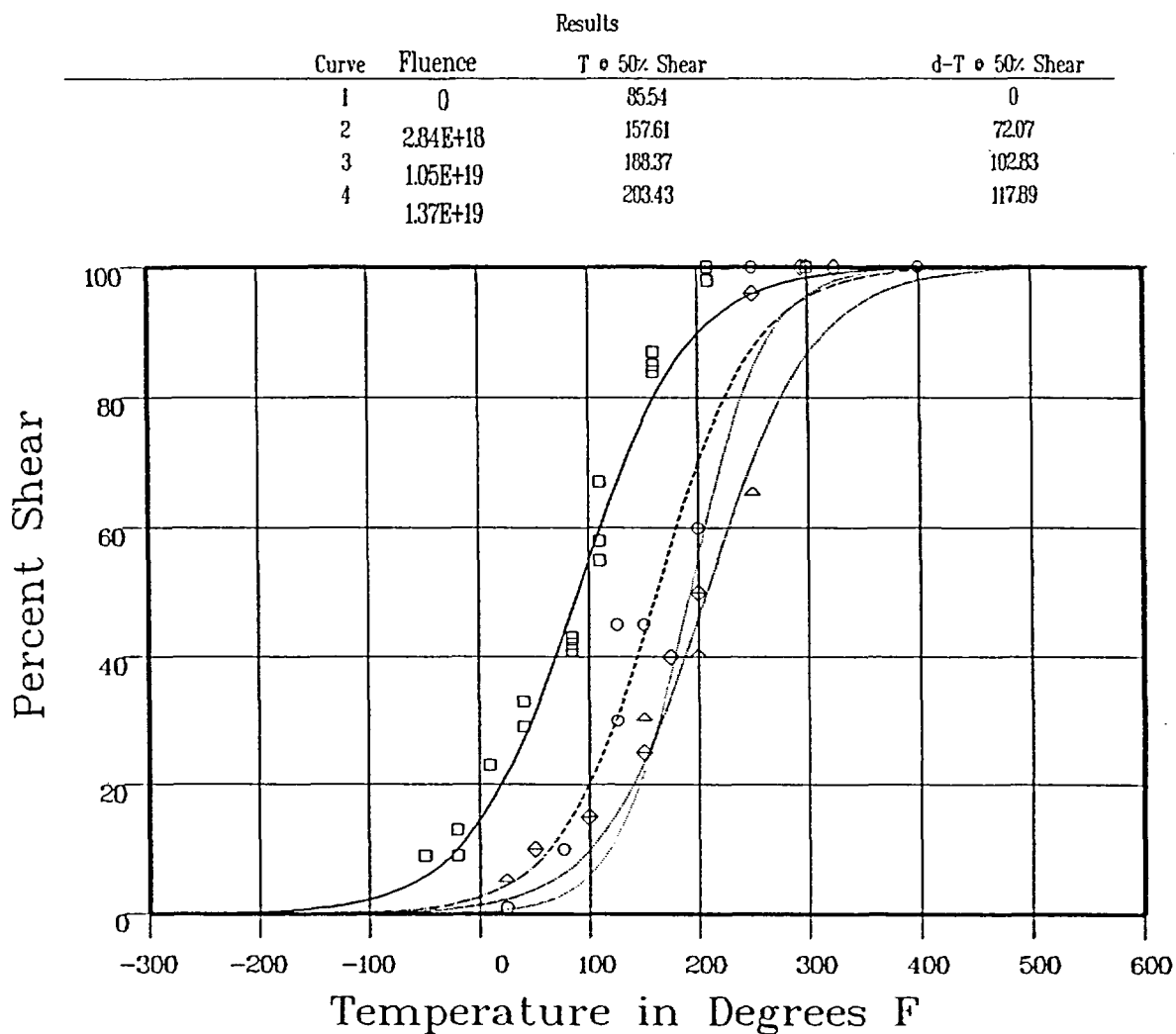
Data Set(s) Plotted

Curve	Plant	Capsule	Material	Ori.	Heat#
1	DCI	UNIRR	SRM SA533B1	LT	
2	DCI	S	SRM SA533B1	LT	
3	DCI	Y	SRM SA533B1	LT	
4	DCI	V	SRM SA533B1	LT	

Figure 5-11 Charpy V-Notch Lateral Expansion vs. Temperature for Diablo Canyon Unit 1 Reactor Vessel Correlation Monitor Material

STANDARD REFERENCE MATERIAL

CVGRAPH 4.1 Hyperbolic Tangent Curve Printed at 11:15:09 on 09-06-2002



Curve Legend

1 □ ——— 2 ○ - - - - - 3 ◇ ——— 4 △ ———

Data Set(s) Plotted

Curve	Plant	Capsule	Material	Ori.	Heat#
1	DCI	UNIRR	SRM SA533B1	LT	
2	DCI	S	SRM SA533B1	LT	
3	DCI	Y	SRM SA533B1	LT	
4	DCI	V	SRM SA533B1	LT	

Figure 5-12 Charpy V-Notch Percent Shear vs. Temperature for Diablo Canyon Unit 1 Reactor Vessel Correlation Monitor Material

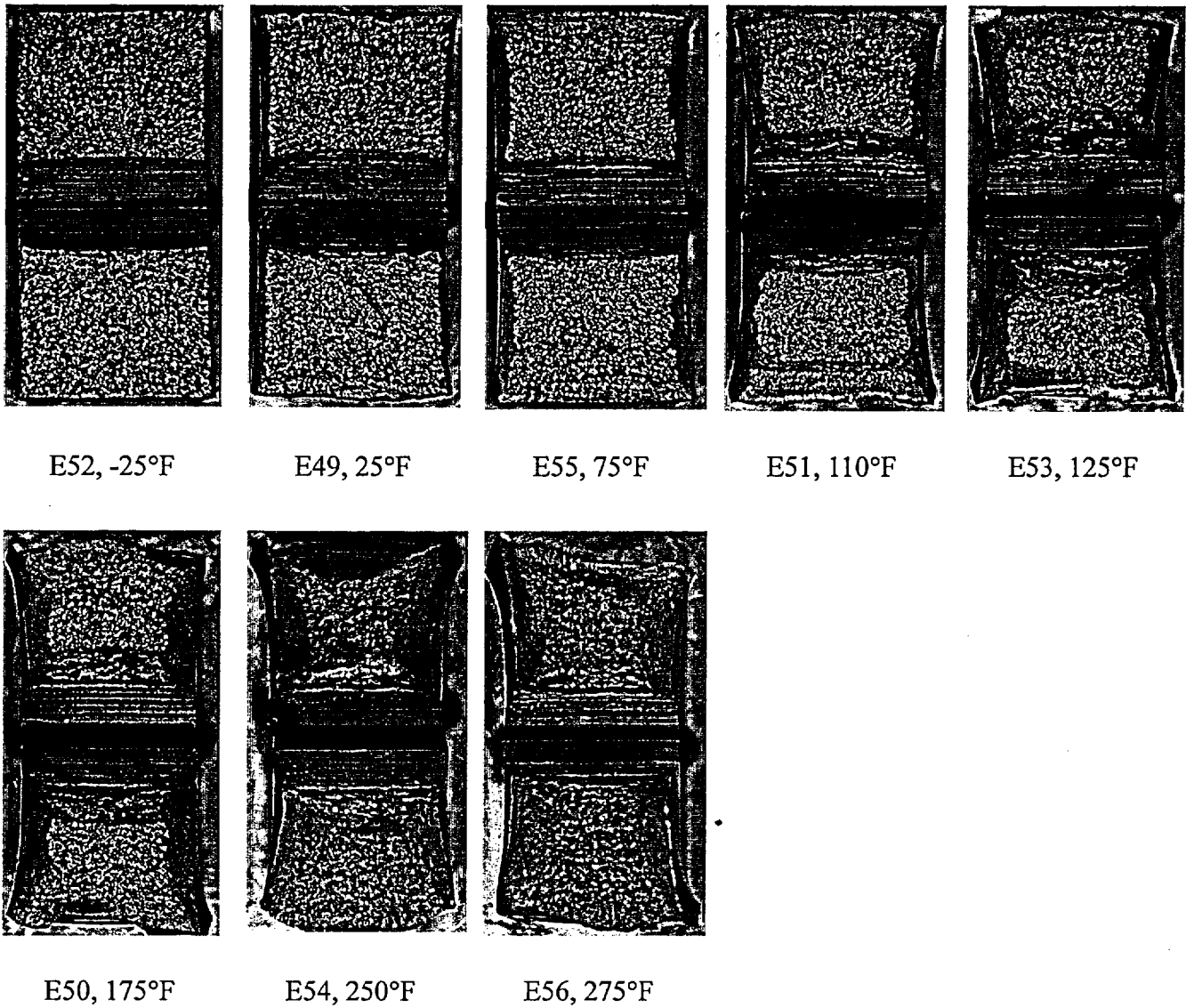


Figure 5-13 Charpy Impact Specimen Fracture Surfaces for Diablo Canyon Unit 1 Reactor Vessel Intermediate Shell Plate B4106-3 (Longitudinal Orientation)

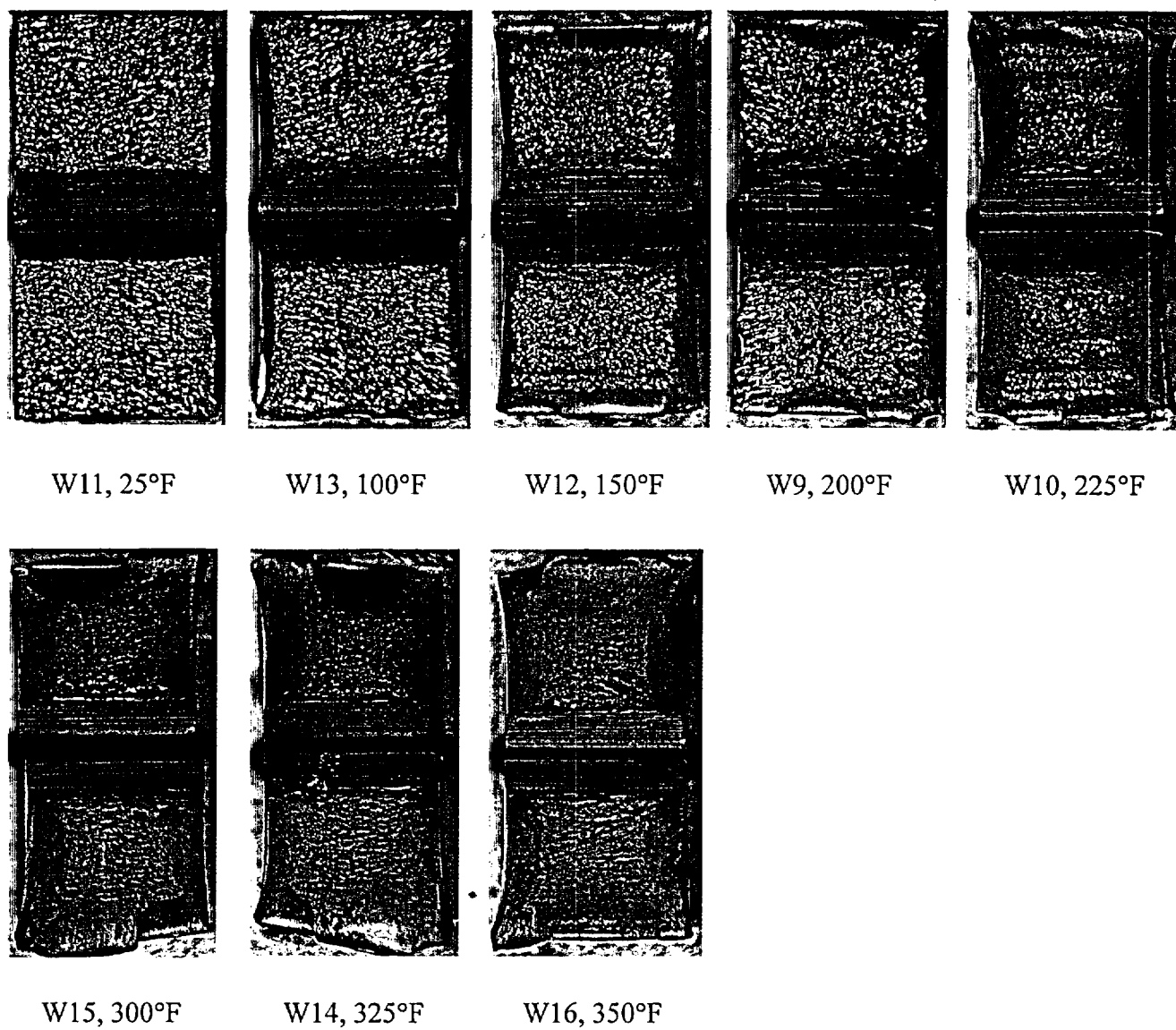


Figure 5-14 Charpy Impact Specimen Fracture Surfaces for Diablo Canyon Unit 1 Reactor Vessel Weld Metal

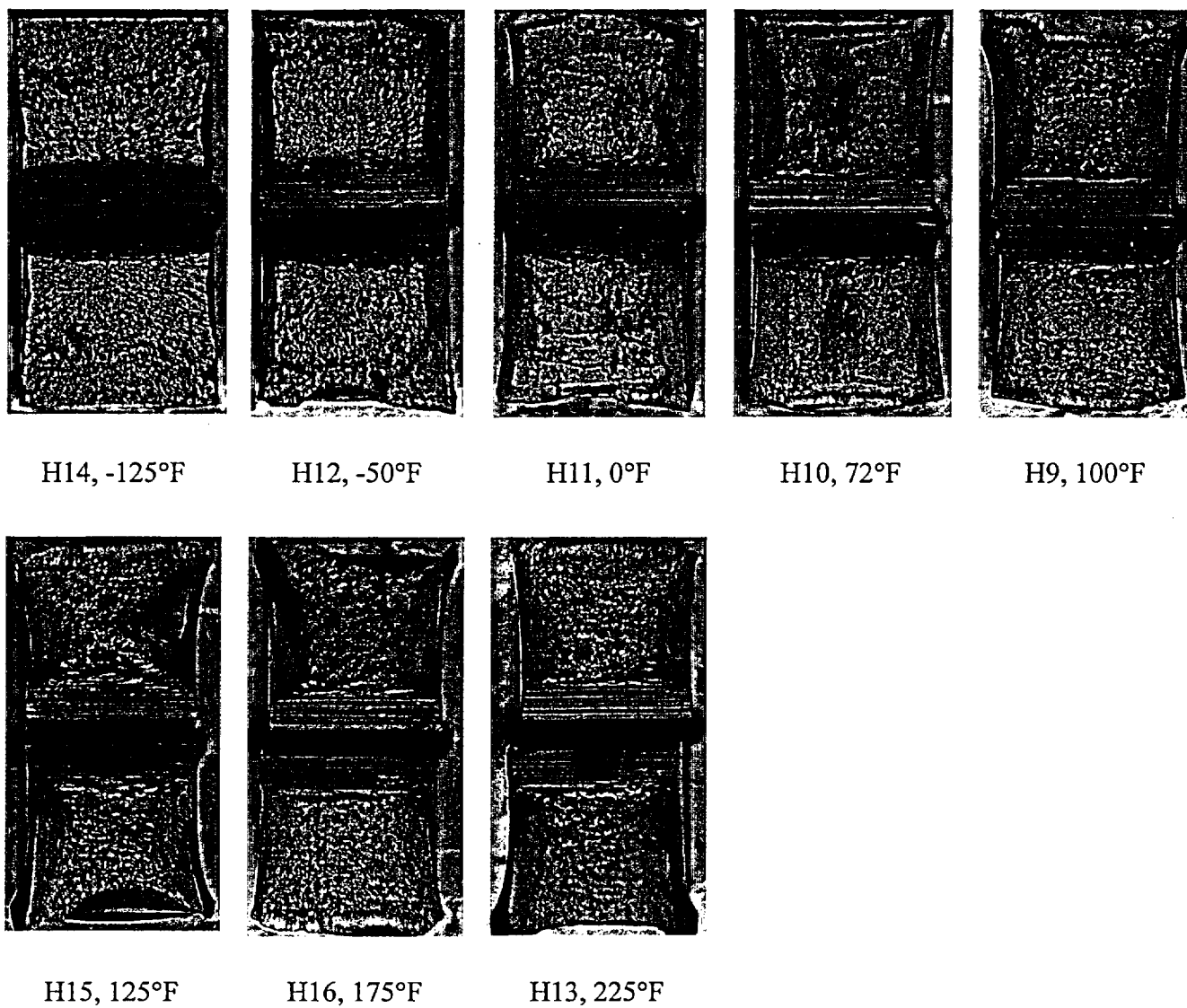
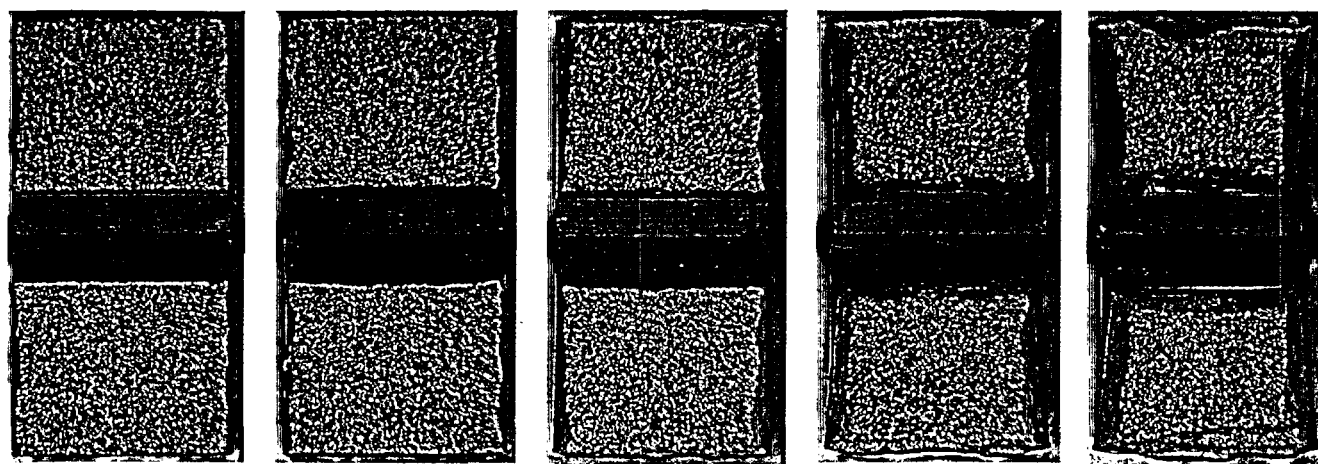


Figure 5-15 Charpy Impact Specimen Fracture Surfaces for Diablo Canyon Unit 1 Reactor Vessel Heat-Affected-Zone Metal



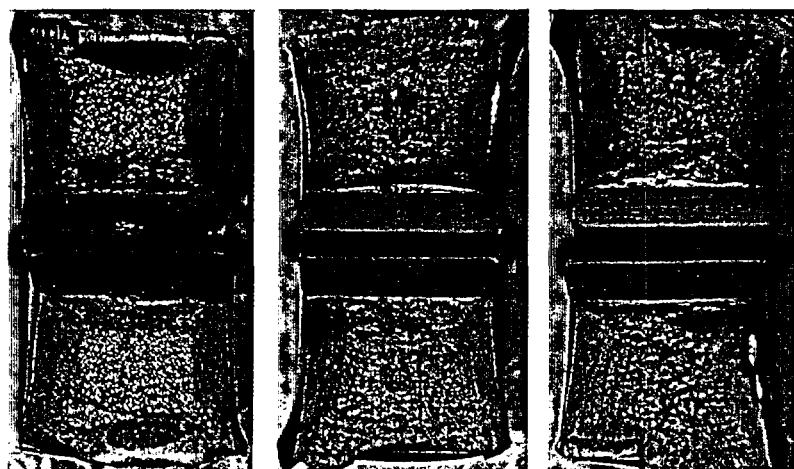
R49, 25°F

R51, 50°F

R56, 100°F

R55, 150°F

R53, 200°F



R54, 250°F

R50, 300°F

R52, 325°F

Figure 5-16 Charpy Impact Specimen Fracture Surfaces for Diablo Canyon Unit 1 Reactor Vessel Correlation Monitor Material

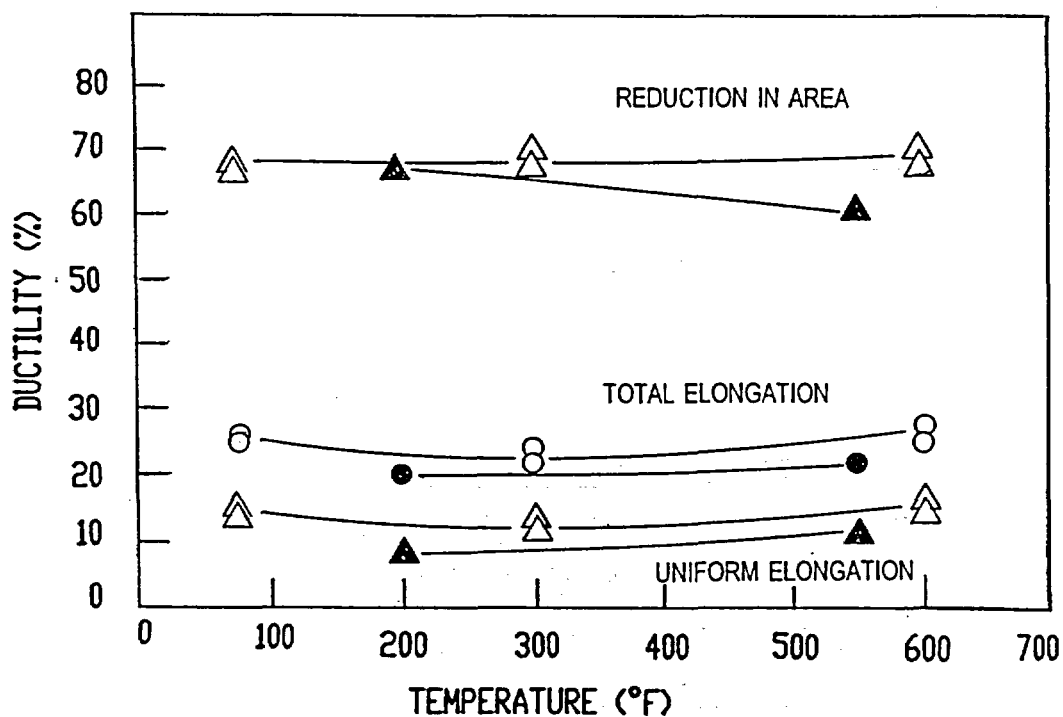
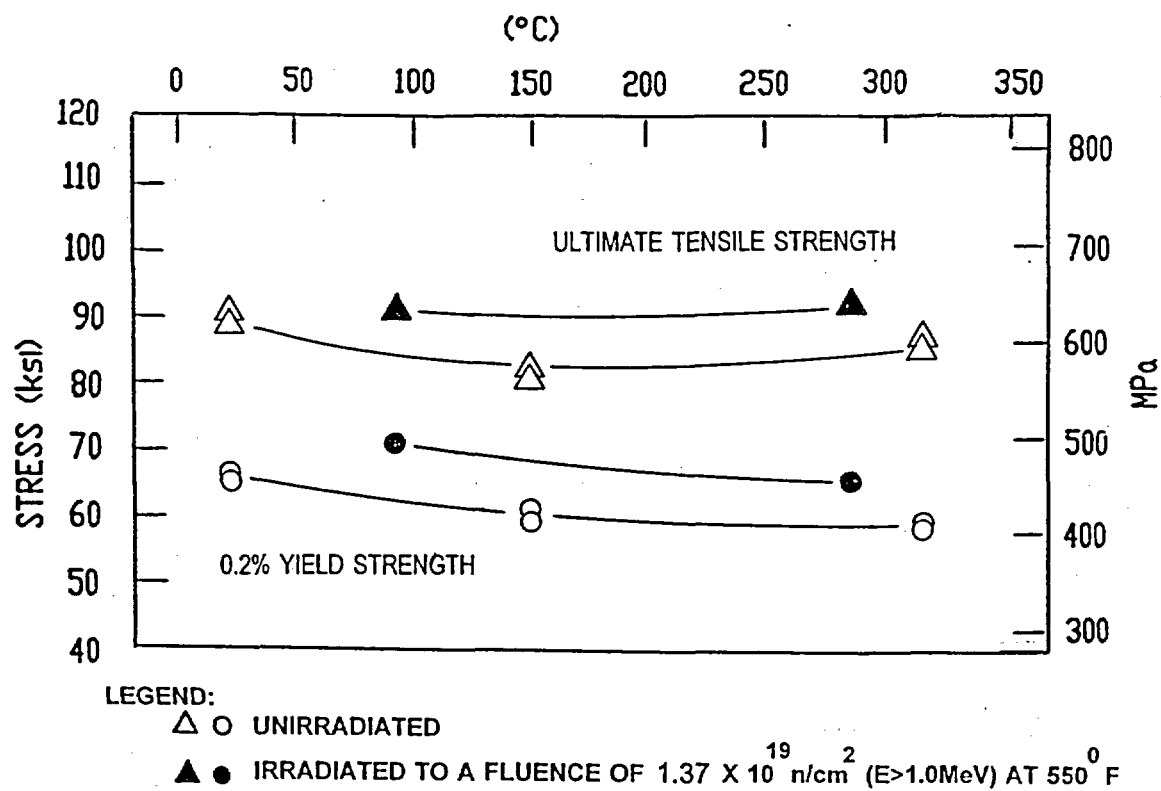


Figure 5-17 Tensile Properties for Diablo Canyon Unit 1 Reactor Vessel Intermediate Shell Plate B4106-3 (Longitudinal Orientation)

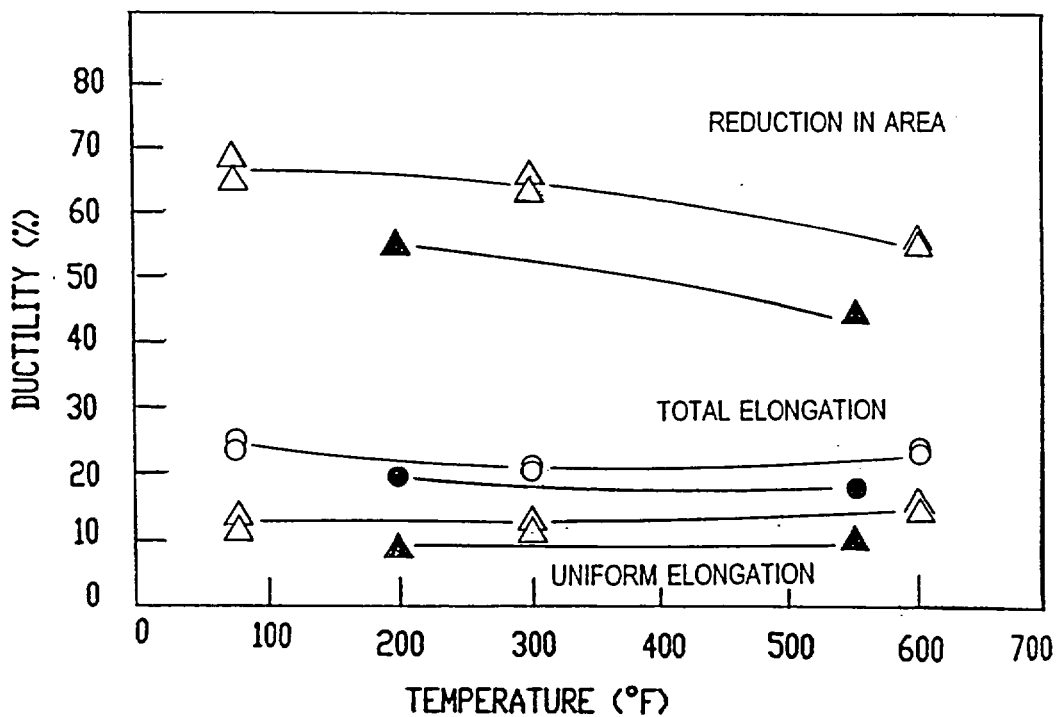
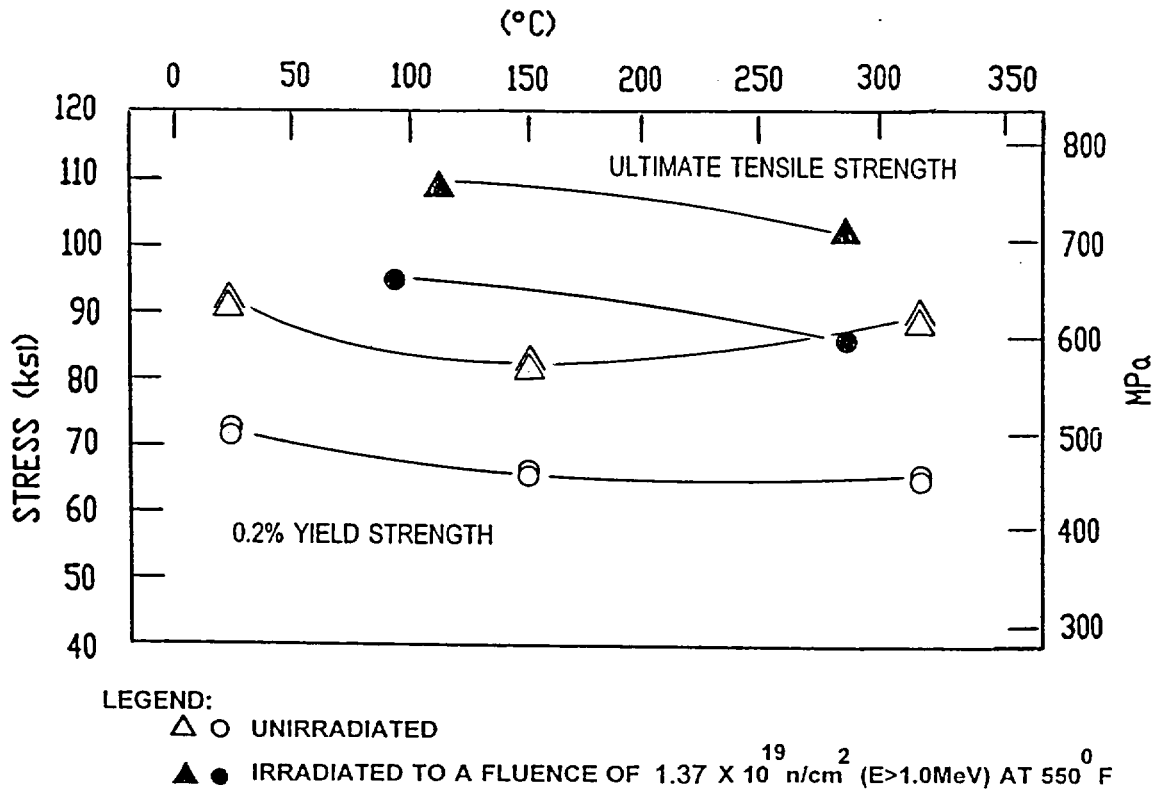
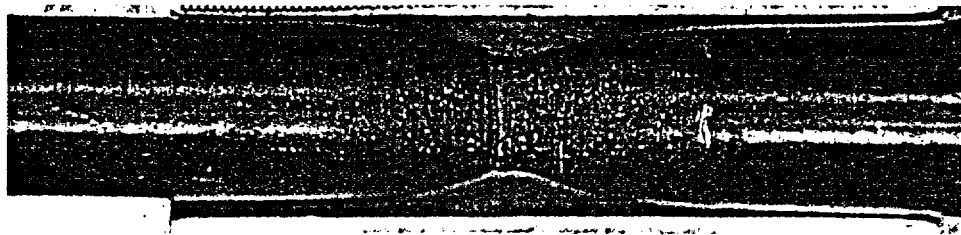
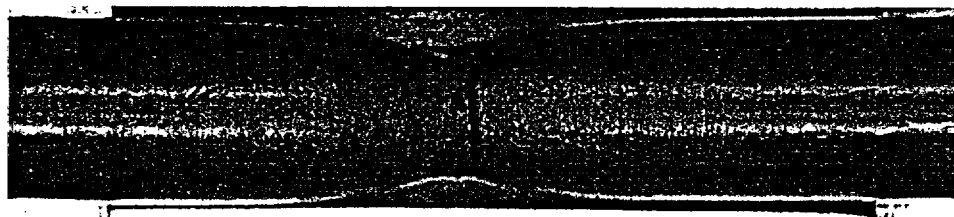


Figure 5-18 Tensile Properties for Diablo Canyon Unit 1 Reactor Vessel Weld Metal

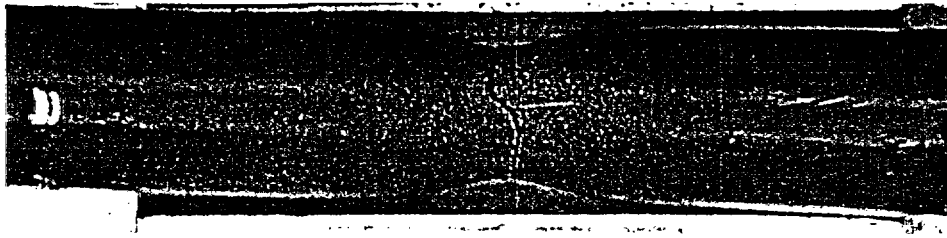


Specimen E8 Tested at 200°F

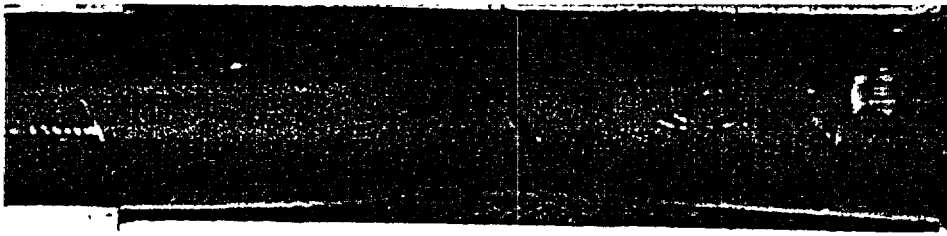


Specimen E9 Tested at 550°F

Figure 5-19 Fractured Tensile Specimens from Diablo Canyon Unit 1 Reactor Vessel Intermediate Shell Plate B4106-3 (Longitudinal Orientation)



Specimen W3 Tested at 200°F



Specimen W4 Tested at 550°F

Figure 5-20 Fractured Tensile Specimens from Diablo Canyon Unit 1 Reactor Vessel Weld Metal

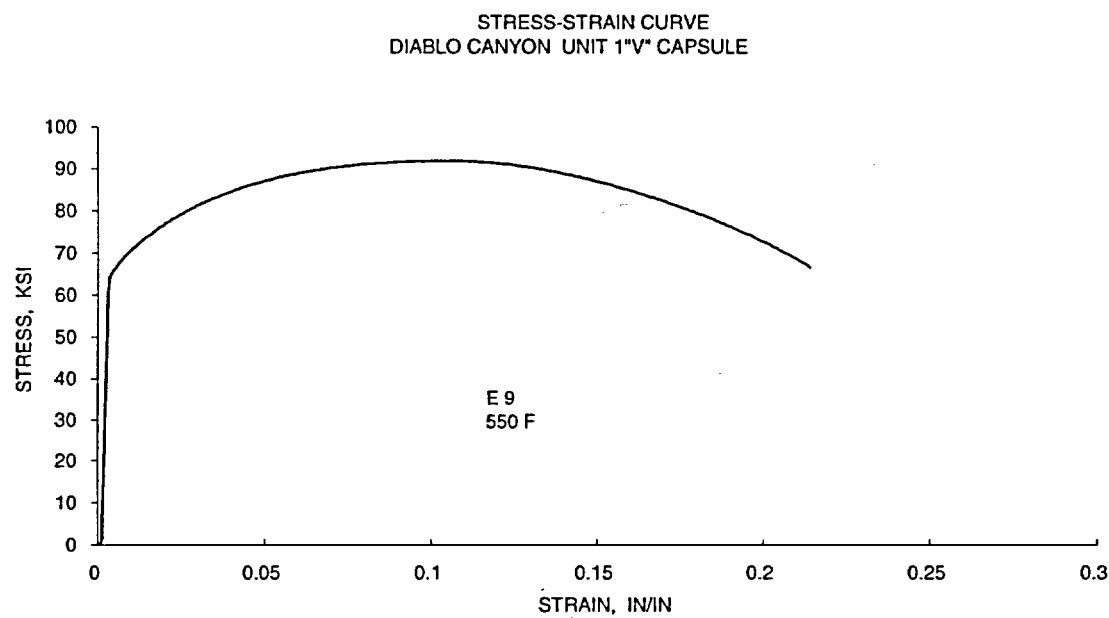
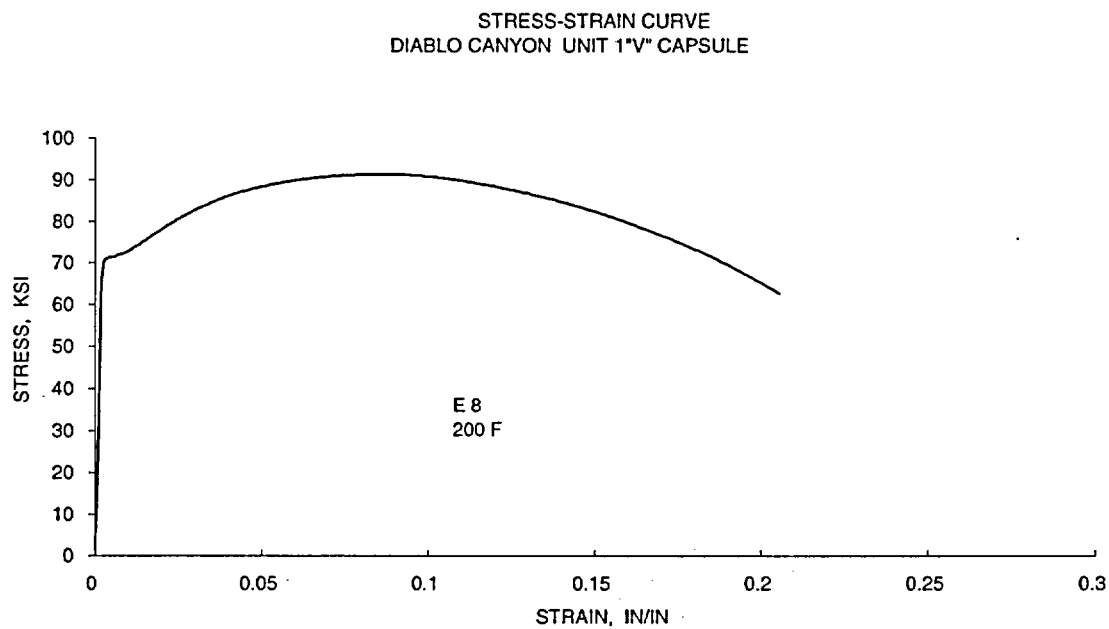


Figure 5-21 Engineering Stress-Strain Curves for Diablo Canyon Unit 1 Intermediate Shell Plate B4106-3 Tensile Specimens E8 and E9 (Longitudinal Orientation)

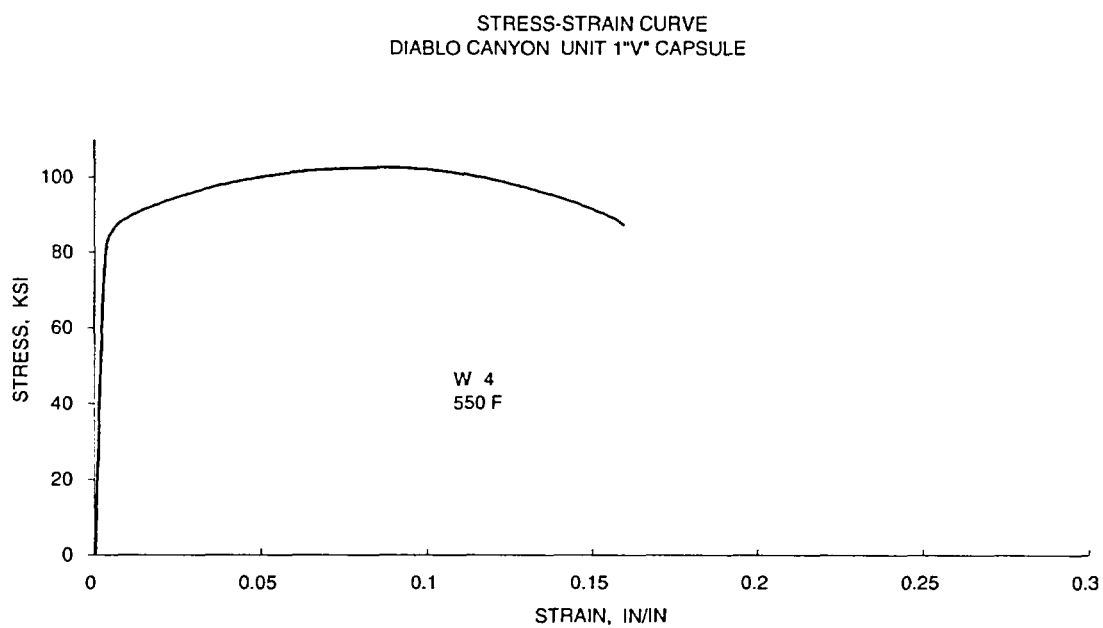
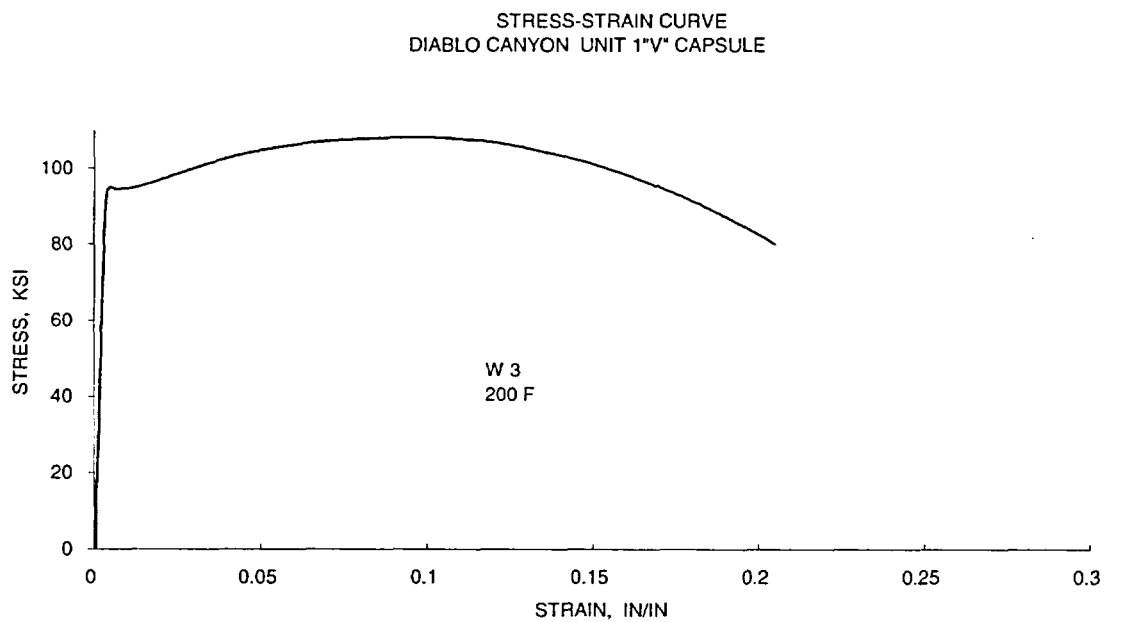


Figure 5-22 Engineering Stress-Strain Curves for Weld Metal Tensile Specimens W3 and W4

6 RADIATION ANALYSIS AND NEUTRON DOSIMETRY

6.1 INTRODUCTION

This section describes a discrete ordinates S_n transport analysis performed for the Diablo Canyon Unit 1 reactor to determine the neutron radiation environment within the reactor pressure vessel and surveillance capsules. In this analysis, fast neutron exposure parameters in terms of fast neutron fluence ($E > 1.0$ MeV) and iron atom displacements (dpa) were established on a plant and fuel cycle specific basis. An evaluation of the most recent dosimetry sensor set from Capsule V, withdrawn at the end of the eleventh plant operating cycle, is provided. In addition, in order to provide a complete measurement database applicable to Diablo Canyon Unit 1, results from prior in-vessel and ex-vessel irradiations are included in Appendix E to this report. The data included in Appendix E were previously documented in Reference 24. Comparisons of the results from these dosimetry evaluations with the analytical predictions served to validate the plant specific neutron transport calculations. These validated calculations subsequently formed the basis for providing projections of the neutron exposure of the reactor pressure vessel for operating periods extending to 54 Effective Full Power Years (EFPY). These projections also account for a plant uprating, from 3338 MWt to 3411 MWt, which began during the eleventh operating cycle.

The use of fast neutron fluence ($E > 1.0$ MeV) to correlate measured material property changes to the neutron exposure of the material has traditionally been accepted for the development of damage trend curves as well as for the implementation of trend curve data to assess the condition of the vessel. In recent years, however, it has been suggested that an exposure model that accounts for differences in neutron energy spectra between surveillance capsule locations and positions within the vessel wall could lead to an improvement in the uncertainties associated with damage trend curves and improved accuracy in the evaluation of damage gradients through the reactor vessel wall.

Because of this potential shift away from a threshold fluence toward an energy dependent damage function for data correlation, ASTM Standard Practice E853, "Analysis and Interpretation of Light-Water Reactor Surveillance Results," recommends reporting displacements per iron atom (dpa) along with fluence ($E > 1.0$ MeV) to provide a database for future reference. The energy dependent dpa function to be used for this evaluation is specified in ASTM Standard Practice E693, "Characterizing Neutron Exposures in Iron and Low Alloy Steels in Terms of Displacements per Atom." The application of the dpa parameter to the assessment of embrittlement gradients through the thickness of the reactor vessel wall has already been promulgated in Revision 2 to Regulatory Guide 1.99, "Radiation Embrittlement of Reactor Vessel Materials."

All of the calculations and dosimetry evaluations described in this section and in Appendix E were based on the latest available nuclear cross-section data derived from ENDF/B-VI and made use of the latest available calculational tools. Furthermore, the neutron transport and dosimetry evaluation methodologies follow the guidance and meet the requirements of Regulatory Guide 1.190, "Calculational and Dosimetry Methods for Determining Pressure Vessel Neutron Fluence."^[19] Additionally, the methods used to develop the calculated pressure vessel fluence are consistent with the NRC approved methodology described in WCAP-14040-NP-A, "Methodology Used to Develop Cold Overpressure Mitigating System Setpoints and RCS Heatup and Cooldown Limit Curves," January 1996.^[20] The specific calculational

methods applied are also consistent with those described in WCAP-15557, "Qualification of the Westinghouse Pressure Vessel Neutron Fluence Evaluation Methodology."^[21]

6.2 DISCRETE ORDINATES ANALYSIS

A plan view of the Diablo Canyon Unit 1 reactor geometry at the core midplane is shown in Figure 4-1. Eight irradiation capsules attached to the thermal shield are included in the reactor design that constitutes the reactor vessel surveillance program. The capsules are located at azimuthal angles of 4°, 176°, 184°, and 356° (4° from the core cardinal axes) and 40°, 140°, 220°, and 320° (40° from the core cardinal axes) as shown in Figure 4-1. The stainless steel specimen containers are 1-inch square by 56 inches in height. The containers are positioned axially such that the test specimens are centered on the core midplane, thus spanning the central 5 feet of the 12-foot high reactor core.

From a neutronic standpoint, the surveillance capsules and associated support structures are significant. The presence of these materials has a marked effect on both the spatial distribution of neutron flux and the neutron energy spectrum in the water annulus between the thermal shield and the reactor vessel. In order to determine the neutron environment at the test specimen location, the capsules themselves must be included in the analytical model.

In performing the fast neutron exposure evaluations for the Diablo Canyon Unit 1 reactor vessel and surveillance capsules, a series of fuel cycle specific forward transport calculations were carried out using the following three-dimensional flux synthesis technique:

$$\phi(r, \theta, z) = \phi(r, \theta) * \frac{\phi(r, z)}{\phi(r)}$$

where $\phi(r, \theta, z)$ is the synthesized three-dimensional neutron flux distribution, $\phi(r, \theta)$ is the transport solution in r, θ geometry, $\phi(r, z)$ is the two-dimensional solution for a cylindrical reactor model using the actual axial core power distribution, and $\phi(r)$ is the one-dimensional solution for a cylindrical reactor model using the same source per unit height as that used in the r, θ two-dimensional calculation. This synthesis procedure was carried out for each operating cycle at Diablo Canyon Unit 1.

For the Diablo Canyon Unit 1 transport calculations, the r, θ model depicted in Figure 6-1 was utilized since the reactor is octant symmetric. This r, θ model includes the core, the reactor internals, the thermal shield -- including explicit representations of the surveillance capsules at 4° and 40°, the pressure vessel cladding and vessel wall, the insulation external to the pressure vessel, and the primary biological shield wall. This model formed the basis for the calculated results and enabled making comparisons to the surveillance capsule dosimetry evaluations. In developing this analytical model, nominal design dimensions were employed for the various structural components. Likewise, water temperatures, and hence, coolant densities in the reactor core and downcomer regions of the reactor were taken to be representative of full power operating conditions. The coolant densities were treated on a fuel cycle specific basis. The reactor core itself was treated as a homogeneous mixture of fuel, cladding, water, and miscellaneous core structures such as fuel assembly grids, guide tubes, et cetera. The geometric mesh

description of the r,θ reactor model consisted of 170 radial by 67 azimuthal intervals. Mesh sizes were chosen to assure that proper convergence of the inner iterations was achieved on a pointwise basis. The pointwise inner iteration flux convergence criterion utilized in the r,θ calculations was set at a value of 0.001.

The r,z model used for the Diablo Canyon Unit 1 calculations that is shown in Figure 6-2 extended radially from the centerline of the reactor core out to a location interior to the primary biological shield and over an axial span from an elevation approximately 1-foot below the active fuel to approximately 1-foot above the active fuel. As in the case of the r,θ model, nominal design dimensions and full power coolant densities were employed in the calculations. In this case, the homogenous core region was treated as an equivalent cylinder with a volume equal to that of the active core zone. The stainless steel former plates located between the core baffle and core barrel regions were also explicitly included in the model. The r,z geometric mesh description of the reactor model consisted of 153 radial by 90 axial intervals. As in the case of the r,θ calculations, mesh sizes were chosen to assure that proper convergence of the inner iterations was achieved on a pointwise basis. The pointwise inner iteration flux convergence criterion utilized in the r,z calculations was also set at a value of 0.001.

The one-dimensional radial model used in the synthesis procedure consisted of the same 153 radial mesh intervals included in the r,z model. Thus, radial synthesis factors could be determined on a meshwise basis throughout the entire geometry.

The core power distributions used in the plant specific transport analysis were taken from the appropriate Diablo Canyon Unit 1 fuel cycle design reports. The data extracted from the design reports represented cycle dependent fuel assembly enrichments, burnups, and axial power distributions. This information was used to develop spatial and energy dependent core source distributions averaged over each individual fuel cycle. Therefore, the results from the neutron transport calculations provided data in terms of fuel cycle averaged neutron flux, which when multiplied by the appropriate fuel cycle length, generated the incremental fast neutron exposure for each fuel cycle. In constructing these core source distributions, the energy distribution of the source was based on an appropriate fission split for uranium and plutonium isotopes based on the initial enrichment and burnup history of individual fuel assemblies. From these assembly dependent fission splits, composite values of energy release per fission, neutron yield per fission, and fission spectrum were determined.

All of the transport calculations supporting this analysis were carried out using the DORT discrete ordinates code Version 3.1^[22] and the BUGLE-96 cross-section library.^[23] The BUGLE-96 library provides a 67 group coupled neutron-gamma ray cross-section data set produced specifically for light water reactor (LWR) applications. In these analyses, anisotropic scattering was treated with a P5 Legendre expansion and angular discretization was modeled with an S16 order of angular quadrature. Energy and space dependent core power distributions, as well as system operating temperatures, were treated on a fuel cycle specific basis.

Selected results from the neutron transport analyses are provided in Tables 6-1 through 6-6. In Table 6-1, the calculated exposure rates and integrated exposures, expressed in terms of both neutron fluence ($E > 1.0$ MeV) and dpa, are given at the radial and azimuthal center of the two azimuthally symmetric surveillance capsule positions (4° and 40°). Also note that Table 6-1 presents calculated exposure rates and integrated exposures for Capsule V, which was irradiated at a 4° location during Cycles 1 through 5,

and subsequently moved to a 40° location until it was removed from service at the end of Cycle 11. These results, representative of the axial midplane of the active core, establish the calculated exposure of the surveillance capsules withdrawn to date as well as projected into the future. Similar information is provided in Table 6-2 for the reactor vessel inner radius. The vessel data given in Table 6-2 are representative of the axial location of the maximum neutron exposure at each of the four azimuthal locations. It is also important to note that the data for the vessel inner radius were taken at the clad/base metal interface, and thus, represent the maximum calculated exposure levels of the vessel forgings and welds.

Both calculated fluence ($E > 1.0$ MeV) and dpa data are provided in Tables 6-1 and 6-2. These data tabulations include both plant and fuel cycle specific calculated neutron exposures at the end of the eleventh operating fuel cycle, as well as projections to 16, 24, 32, 40, 48, and 54 effective full power years (EFPY). The projections were based on the assumption that the radial power distribution averaged from fuel cycles 5-11 was representative of future plant operation. All remaining core parameters were obtained by averaging cycles 5-11. The future projections are also based on the current reactor power level of 3411 MWt.

Radial gradient information applicable to fast ($E > 1.0$ MeV) neutron fluence and dpa are given in Tables 6-3 and 6-4, respectively. The data, based on the cumulative integrated exposures from Cycles 1 through 11, are presented on a relative basis for each exposure parameter at several azimuthal locations. Exposure distributions through the vessel wall may be obtained by multiplying the calculated exposure at the vessel inner radius by the gradient data listed in Tables 6-3 and 6-4.

The calculated fast neutron exposures for the three surveillance capsules withdrawn from the Diablo Canyon Unit 1 reactor are provided in Table 6-5. These assigned neutron exposure levels are based on the plant and fuel cycle specific neutron transport calculations performed for the Diablo Canyon Unit 1 reactor.

Updated lead factors for the Diablo Canyon Unit 1 surveillance capsules are provided in Table 6-6. The capsule lead factor is defined as the ratio of the calculated fluence ($E > 1.0$ MeV) at the geometric center of the surveillance capsule to the corresponding maximum calculated fluence at the pressure vessel clad/base metal interface. In Table 6-6, the lead factors for capsules that have been withdrawn from the reactor (S, Y, and V) were based on the calculated fluence values for the irradiation period corresponding to the time of withdrawal for the individual capsules. For the capsules remaining in the reactor (U, W, X, A, B, C, and D), the lead factors correspond to the calculated fluence values at the end of 54 effective full power years (EFPY).

6.3 NEUTRON DOSIMETRY

The validity of the calculated neutron exposures previously reported in Section 6.2 is demonstrated by a direct comparison against the measured sensor reaction rates and via a least squares evaluation performed for each of the capsule dosimetry sets. However, since the neutron dosimetry measurement data merely serves to validate the calculated results, only the direct comparison of measured-to-calculated results for the most recent surveillance capsule removed from service is provided in this section of the report. For completeness, the assessment of all measured dosimetry removed to date, based on direct, best estimate, and least squares evaluation comparisons, is documented in Appendix E.

The direct comparison of measured versus calculated fast neutron threshold reaction rates for the sensors from Capsule V that was withdrawn from Diablo Canyon Unit 1 at the end of the eleventh fuel cycle, is summarized below.

Reaction	Reaction Rates (rps/atom)		M/C Ratio
	Measured	Calculated	
$^{63}\text{Cu}(n,\alpha)^{60}\text{Co}$	2.26E-17	2.32E-17	0.97
$^{54}\text{Fe}(n,p)^{54}\text{Mn}$	1.81E-15	2.32E-15	0.78
$^{58}\text{Ni}(n,p)^{58}\text{Co}$	2.85E-15	2.77E-15	0.90
$^{238}\text{U}(n,p)^{137}\text{Cs}$ (Cd)	8.84E-15	9.24E-14	0.82
$^{237}\text{Np}(n,f)^{137}\text{Cs}$ (Cd)	7.82E-14	7.39E-14	0.97
Average:			0.89
% Standard Deviation:			9.8

The measured-to-calculated (M/C) reaction rate ratios for the Capsule V threshold reactions range from 0.78 to 0.97, and the average M/C ratio is $0.89 \pm 9.8\%$ (1σ). This direct comparison falls well within the $\pm 20\%$ criterion specified in Regulatory Guide 1.190; furthermore, it is consistent with the full set of comparisons given in Appendix E for all measured dosimetry removed to date from the Diablo Canyon Unit 1 reactor. As a result, these comparisons validate the current analytical results described in Section 6.2 which are deemed applicable for Diablo Canyon Unit 1.

6.4 CALCULATIONAL UNCERTAINTIES

The uncertainty associated with the calculated neutron exposure of the Diablo Canyon Unit 1 surveillance capsule and reactor pressure vessel is based on the recommended approach provided in Regulatory Guide 1.190. In particular, the qualification of the methodology was carried out in the following four stages:

1. Comparison of calculations with benchmark measurements from the Pool Critical Assembly (PCA) simulator at the Oak Ridge National Laboratory (ORNL).
2. Comparisons of calculations with surveillance capsule and reactor cavity measurements from the H. B. Robinson power reactor benchmark experiment.
3. An analytical sensitivity study addressing the uncertainty components resulting important input parameters applicable to the plant specific transport calculations used in the neutron exposure assessments.
4. Comparisons of the plant specific calculations with all available dosimetry results from the Diablo Canyon Unit 1 surveillance program.

The first phase of the methods qualification (PCA comparisons) addressed the adequacy of basic transport calculation and dosimetry evaluation techniques and associated cross-sections. This phase, however, did not test the accuracy of commercial core neutron source calculations nor did it address uncertainties in operational or geometric variables that impact power reactor calculations. The second phase of the qualification (H. B. Robinson comparisons) addressed uncertainties in these additional areas that are primarily methods related and would tend to apply generically to all fast neutron exposure evaluations. The third phase of the qualification (analytical sensitivity study) identified the potential uncertainties introduced into the overall evaluation due to calculational methods approximations as well as to a lack of knowledge relative to various plant specific input parameters. The overall calculational uncertainty applicable to the Diablo Canyon Unit 1 analysis was established from results of these three phases of the methods qualification.

The fourth phase of the uncertainty assessment (comparisons with Diablo Canyon Unit 1 measurements) was used solely to demonstrate the validity of the transport calculations and to confirm the uncertainty estimates associated with the analytical results. The comparison was used only as a check and was not used in any way to modify the calculated surveillance capsule and pressure vessel neutron exposures previously described in Section 6.2. As such, the validation of the Diablo Canyon Unit 1 analytical model based on the measured plant dosimetry is completely described in Appendix E.

The following summarizes the uncertainties developed from the first three phases of the methodology qualification. Additional information pertinent to these evaluations is provided in Reference 21.

	Capsule	Vessel IR
PCA Comparisons	3%	3%
H. B. Robinson Comparisons	3%	3%
Analytical Sensitivity Studies	10%	11%
Additional Uncertainty for Factors not Explicitly Evaluated	5%	5%
Net Calculational Uncertainty	12%	13%

The net calculational uncertainty was determined by combining the individual components in quadrature. Therefore, the resultant uncertainty was random and no systematic bias was applied to the analytical results.

The plant specific measurement comparisons described in Appendix E support these uncertainty assessments for Diablo Canyon Unit 1.

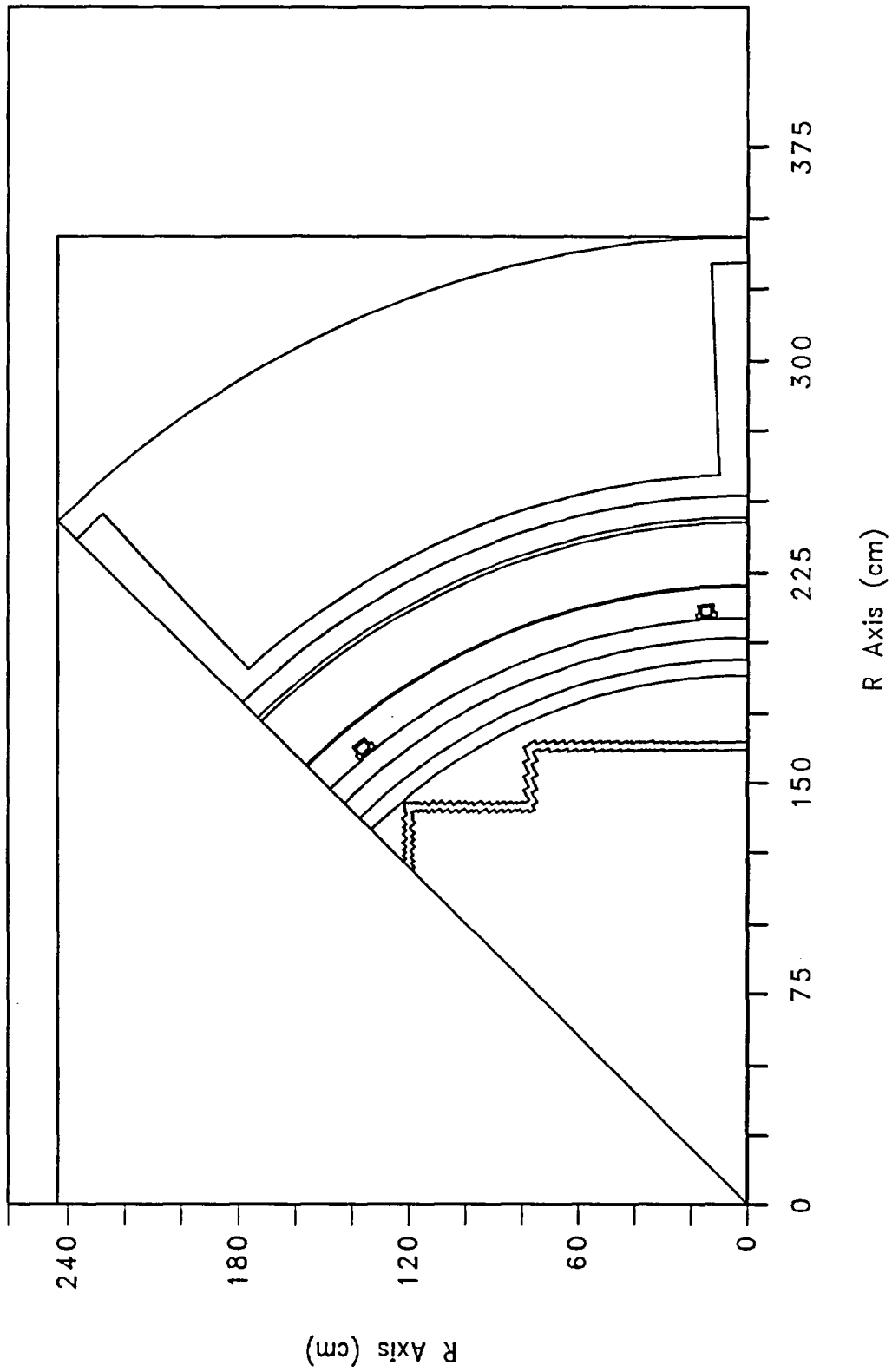


Figure 6-1 Diablo Canyon Unit 1 r,θ Reactor Geometry at the Core Midplane

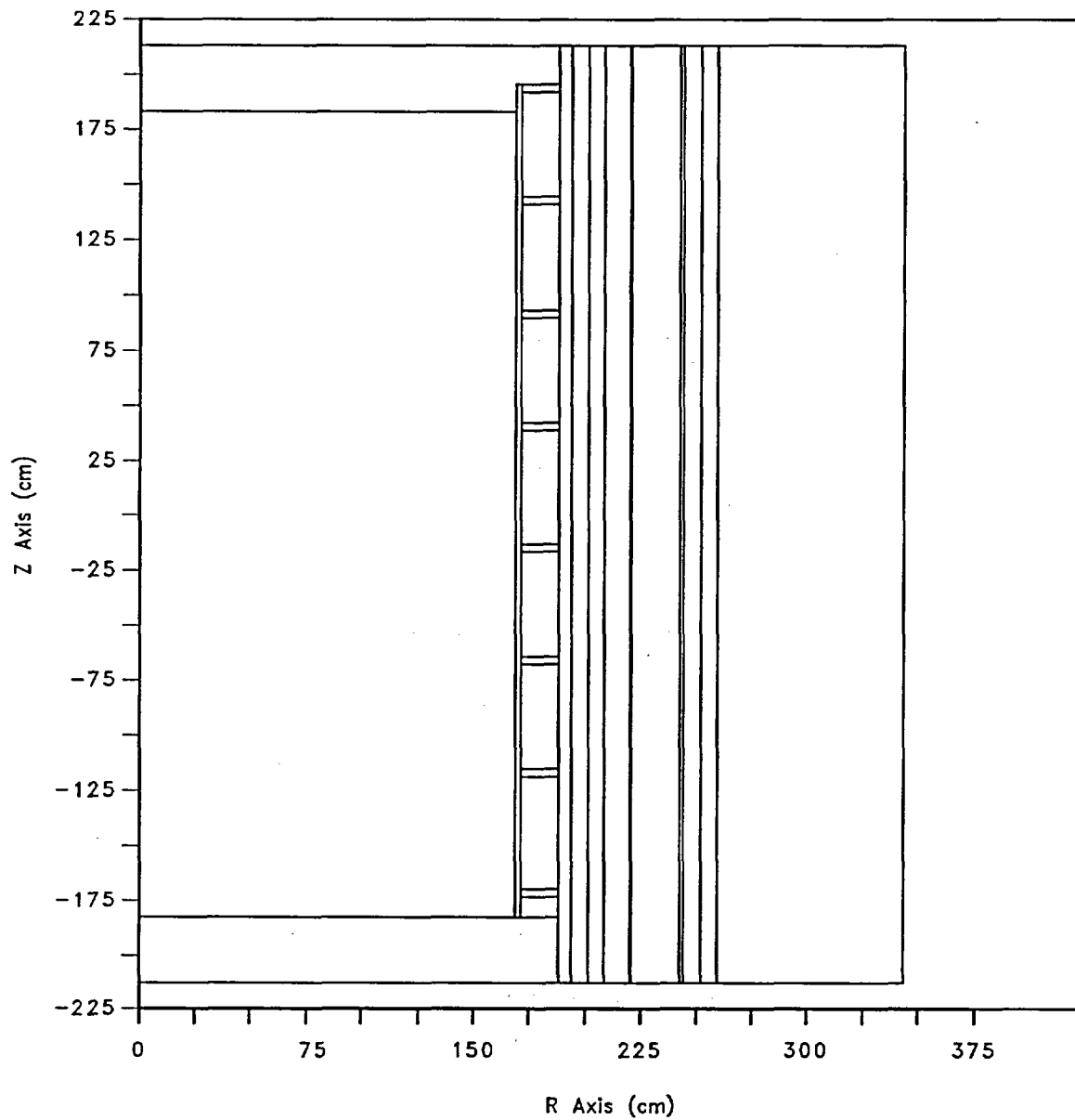


Figure 6-2 Diablo Canyon Unit 1 r,z Reactor Geometry

Table 6-1
Calculated Neutron Exposure Rates and Integrated Exposures

At The Surveillance Capsule Center

Neutrons (E > 1.0 MeV)

Cycle	Cycle Length [EFPS]	Cumulative Irradiation Time [EFPS]	Cumulative Irradiation Time [EFPY]	Neutron Flux (E > 1.0 MeV) [n/cm ² -s]		
				4°	40°	4° → 40° (Cap. V*)
1	3.94E+07	3.94E+07	1.25	2.24E+10	7.23E+10	2.24E+10
2	3.23E+07	7.16E+07	2.27	1.94E+10	6.03E+10	1.94E+10
3	3.72E+07	1.09E+08	3.45	1.60E+10	6.28E+10	1.60E+10
4	3.34E+07	1.42E+08	4.51	1.63E+10	4.85E+10	1.63E+10
5	4.31E+07	1.85E+08	5.87	1.54E+10	4.14E+10	1.54E+10
6	4.01E+07	2.25E+08	7.14	1.61E+10	4.16E+10	4.16E+10
7	4.18E+07	2.67 E+08	8.47	1.56E+10	4.11E+10	4.11E+10
8	4.04E+07	3.08 E+08	9.75	1.37E+10	3.69E+10	3.69E+10
9	5.13E+07	3.59 E+08	11.38	1.51E+10	3.87E+10	3.87E+10
10	4.72E+07	4.06 E+08	12.87	1.36E+10	3.80E+10	3.80E+10
11	4.58E+07	4.52 E+08	14.27	1.49E+10	3.84E+10	3.84E+10
Projection	5.29E+07	5.05 E+08	16.00	1.52E+10	4.02E+10	4.02E+10
Projection	2.53E+08	7.57 E+08	24.00	1.52E+10	4.02E+10	4.02E+10
Projection	2.53E+08	1.01E+09	32.00	1.52E+10	4.02E+10	4.02E+10
Projection	2.53E+08	1.26E+09	40.00	1.52E+10	4.02E+10	4.02E+10
Projection	2.53E+08	1.51E+09	48.00	1.52E+10	4.02E+10	4.02E+10
Projection	1.89E+08	1.70E+09	54.00	1.52E+10	4.02E+10	4.02E+10

Note: Neutron exposure values reported for the surveillance capsules are centered at the core midplane.

* Capsule V was irradiated at a 4° location during Cycles 1 through 5 followed by a 40° location during Cycles 6 through 11 when it was subsequently removed from service.

Table 6-1 cont'd

Calculated Neutron Exposure Rates and Integrated Exposures

At The Surveillance Capsule Center

Neutrons ($E > 1.0$ MeV)

Cycle	Cycle Length [EFPS]	Cumulative Irradiation Time [EFPS]	Cumulative Irradiation Time [EFPY]	Neutron Fluence ($E > 1.0$ MeV) [n/cm ²]		
				4°	40°	4° → 40° (Cap. V*)
1	3.94E+07	3.94E+07	1.25	8.82E+17	2.84E+18	8.82E+17
2	3.23E+07	7.16E+07	2.27	1.51E+18	4.79E+18	1.51E+18
3	3.72E+07	1.09E+08	3.45	2.10E+18	7.13E+18	2.10E+18
4	3.34E+07	1.42E+08	4.51	2.65E+18	8.75E+18	2.65E+18
5	4.31E+07	1.85E+08	5.87	3.31E+18	1.05E+19	3.31E+18
6	4.01E+07	2.25E+08	7.14	3.96E+18	1.22E+19	4.98E+18
7	4.18E+07	2.67E+08	8.47	4.61E+18	1.39E+19	6.69E+18
8	4.04E+07	3.08E+08	9.75	5.16E+18	1.54E+19	8.18E+18
9	5.13E+07	3.59E+08	11.38	5.93E+18	1.74E+19	1.02E+19
10	4.72E+07	4.06E+08	12.87	6.58E+18	1.92E+19	1.20E+19
11	4.58E+07	4.52E+08	14.27	7.26E+18	2.09E+19	1.37E+19
Projection	5.29E+07	5.05E+08	16.00	8.06E+18	2.31E+19	1.58E+19
Projection	2.53E+08	7.57E+08	24.00	1.19E+19	3.32E+19	2.60E+19
Projection	2.53E+08	1.01E+09	32.00	1.57E+19	4.33E+19	3.61E+19
Projection	2.53E+08	1.26E+09	40.00	1.96E+19	5.35E+19	4.63E+19
Projection	2.53E+08	1.51E+09	48.00	2.34E+19	6.36E+19	5.64E+19
Projection	1.89E+08	1.70E+09	54.00	2.63E+19	7.12E+19	6.40E+19

Note: Neutron exposure values reported for the surveillance capsules are centered at the core midplane.

* Capsule V was irradiated at a 4° location during Cycles 1 through 5 followed by a 40° location during Cycles 6 through 11 when it was subsequently removed from service.

Table 6-1 cont'd

Calculated Neutron Exposure Rates and Integrated Exposures

At The Surveillance Capsule Center

Iron Atom Displacements

Cycle	Cycle Length [EFPS]	Cumulative Irradiation Time [EFPS]	Cumulative Irradiation Time [EFPY]	Displacement Rate [dpa/s]		
				4°	40°	4° → 40° (Cap. V*)
1	3.94E+07	3.94E+07	1.25	3.61E-11	1.22E-10	3.61E-11
2	3.23E+07	7.16E+07	2.27	3.12E-11	1.02E-10	3.12E-11
3	3.72E+07	1.09E+08	3.45	2.57E-11	1.06E-10	2.57E-11
4	3.34E+07	1.42E+08	4.51	2.63E-11	8.14E-11	2.63E-11
5	4.31E+07	1.85E+08	5.87	2.48E-11	6.95E-11	2.48E-11
6	4.01E+07	2.25E+08	7.14	2.60E-11	6.98E-11	6.98E-11
7	4.18E+07	2.67E+08	8.47	2.51E-11	6.90E-11	6.90E-11
8	4.04E+07	3.08E+08	9.75	2.20E-11	6.19E-11	6.19E-11
9	5.13E+07	3.59E+08	11.38	2.43E-11	6.50E-11	6.50E-11
10	4.72E+07	4.06E+08	12.87	2.20E-11	6.37E-11	6.37E-11
11	4.58E+07	4.52E+08	14.27	2.39E-11	6.45E-11	6.45E-11
Projection	5.29E+07	5.05E+08	16.00	2.45E-11	6.74E-11	6.74E-11
Projection	2.53E+08	7.57E+08	24.00	2.45E-11	6.74E-11	6.74E-11
Projection	2.53E+08	1.01E+09	32.00	2.45E-11	6.74E-11	6.74E-11
Projection	2.53E+08	1.26E+09	40.00	2.45E-11	6.74E-11	6.74E-11
Projection	2.53E+08	1.51E+09	48.00	2.45E-11	6.74E-11	6.74E-11
Projection	1.89E+08	1.70E+09	54.00	2.45E-11	6.74E-11	6.74E-11

Note: Neutron exposure values reported for the surveillance capsules are centered at the core midplane.

* Capsule V was irradiated at a 4° location during Cycles 1 through 5 followed by a 40° location during Cycles 6 through 11 when it was subsequently removed from service.

Table 6-1 cont'd

Calculated Neutron Exposure Rates and Integrated Exposures

At The Surveillance Capsule Center

Iron Atom Displacements

Cycle	Cycle Length [EFPS]	Cumulative Irradiation Time [EFPS]	Cumulative Irradiation Time [EFPY]	Displacements [dpa]		
				4°	40°	4° → 40° (Cap. V*)
1	3.94E+07	3.94E+07	1.25	1.42E-03	4.80E-03	1.42E-03
2	3.23E+07	7.16E+07	2.27	2.43E-03	8.08E-03	2.43E-03
3	3.72E+07	1.09E+08	3.45	3.39E-03	1.20E-02	3.39E-03
4	3.34E+07	1.42E+08	4.51	4.26E-03	1.47E-02	4.26E-03
5	4.31E+07	1.85E+08	5.87	5.33E-03	1.77E-02	5.33E-03
6	4.01E+07	2.25E+08	7.14	6.37E-03	2.05E-02	8.13E-03
7	4.18E+07	2.67 E+08	8.47	7.42E-03	2.34E-02	1.10E-02
8	4.04E+07	3.08 E+08	9.75	8.31E-03	2.59E-02	1.35E-02
9	5.13E+07	3.59 E+08	11.38	9.56E-03	2.92E-02	1.69E-02
10	4.72E+07	4.06 E+08	12.87	1.06E-02	3.23E-02	1.99E-02
11	4.58E+07	4.52 E+08	14.27	1.17E-02	3.52E-02	2.28E-02
Projection	5.29E+07	5.05 E+08	16.00	1.30E-02	3.88E-02	2.64E-02
Projection	2.53E+08	7.57 E+08	24.00	1.92E-02	5.58E-02	4.34E-02
Projection	2.53E+08	1.01E+09	32.00	2.54E-02	7.28E-02	6.04E-02
Projection	2.53E+08	1.26E+09	40.00	3.16E-02	8.99E-02	7.75E-02
Projection	2.53E+08	1.51E+09	48.00	3.77E-02	1.07E-01	9.45E-02
Projection	1.89E+08	1.70E+09	54.00	4.24E-02	1.20E-01	1.07E-01

Note: Neutron exposure values reported for the surveillance capsules are centered at the core midplane.

* Capsule V was irradiated at a 4° location during Cycles 1 through 5 followed by a 40° location during Cycles 6 through 11 when it was subsequently removed from service.

Table 6-2
Calculated Azimuthal Variation of Maximum Exposure Rates
And Integrated Exposures at the Reactor Vessel
Clad/Base Metal Interface

Cycle	Cycle Length [EFPS]	Cumulative Irradiation Time [EFPS]	Cumulative Irradiation Time [EFPY]	Neutron Flux (E > 1.0 MeV) [n/cm ² -s]			
				0°	15°	30°	45°
1	3.94E+07	3.94E+07	1.25	6.75E+09	1.07E+10	1.35E+10	2.08E+10
2	3.23E+07	7.16E+07	2.27	5.93E+09	8.45E+09	1.16E+10	1.75E+10
3	3.72E+07	1.09E+08	3.45	4.83E+09	7.87E+09	1.19E+10	1.82E+10
4	3.34E+07	1.42E+08	4.51	4.94E+09	7.57E+09	9.54E+09	1.43E+10
5	4.31E+07	1.85E+08	5.87	4.67E+09	7.06E+09	8.80E+09	1.20E+10
6	4.01E+07	2.25E+08	7.14	4.88E+09	7.65E+09	8.87E+09	1.21E+10
7	4.18E+07	2.67 E+08	8.47	4.70E+09	7.56E+09	8.99E+09	1.19E+10
8	4.04E+07	3.08 E+08	9.75	4.19E+09	6.86E+09	8.24E+09	1.08E+10
9	5.13E+07	3.59 E+08	11.38	4.58E+09	6.99E+09	8.40E+09	1.12E+10
10	4.72E+07	4.06 E+08	12.87	4.08E+09	7.26E+09	8.74E+09	1.10E+10
11	4.58E+07	4.52 E+08	14.27	4.42E+09	8.20E+09	9.48E+09	1.10E+10
Projection	5.29E+07	5.05 E+08	16.00	4.59E+09	7.52E+09	8.96E+09	1.16E+10
Projection	2.53E+08	7.57 E+08	24.00	4.59E+09	7.52E+09	8.96E+09	1.16E+10
Projection	2.53E+08	1.01E+09	32.00	4.59E+09	7.52E+09	8.96E+09	1.16E+10
Projection	2.53E+08	1.26E+09	40.00	4.59E+09	7.52E+09	8.96E+09	1.16E+10
Projection	2.53E+08	1.51E+09	48.00	4.59E+09	7.52E+09	8.96E+09	1.16E+10
Projection	1.89E+08	1.70E+09	54.00	4.59E+09	7.52E+09	8.96E+09	1.16E+10

Table 6-2 cont'd

Calculated Azimuthal Variation of Maximum Exposure Rates

And Integrated Exposures at the Reactor Vessel

Clad/Base Metal Interface

Cycle	Cycle Length [EFPS]	Cumulative Irradiation Time [EFPS]	Cumulative Irradiation Time [EFPY]	Neutron Fluence (E > 1.0 MeV) [n/cm ²]			
				0°	15°	30°	45°
1	3.94E+07	3.94E+07	1.25	2.66E+17	4.21E+17	5.33E+17	8.20E+17
2	3.23E+07	7.16E+07	2.27	4.57E+17	6.93E+17	9.07E+17	1.38 E+18
3	3.72E+07	1.09E+08	3.45	6.37E+17	9.86E+17	1.35 E+18	2.06 E+18
4	3.34E+07	1.42E+08	4.51	8.01E+17	1.24 E+18	1.67 E+18	2.54 E+18
5	4.31E+07	1.85E+08	5.87	1.00E+18	1.54 E+18	2.05 E+18	3.06 E+18
6	4.01E+07	2.25E+08	7.14	1.20 E+18	1.85 E+18	2.40 E+18	3.54 E+18
7	4.18E+07	2.67 E+08	8.47	1.39 E+18	2.17 E+18	2.78 E+18	4.04 E+18
8	4.04E+07	3.08 E+08	9.75	1.56 E+18	2.44 E+18	3.11 E+18	4.47 E+18
9	5.13E+07	3.59 E+08	11.38	1.80 E+18	2.80 E+18	3.54 E+18	5.05 E+18
10	4.72E+07	4.06 E+08	12.87	1.99 E+18	3.14 E+18	3.95 E+18	5.56 E+18
11	4.58E+07	4.52 E+08	14.27	2.19 E+18	3.52 E+18	4.39 E+18	6.07 E+18
Projection	5.29E+07	5.05 E+08	16.00	2.44 E+18	3.91 E+18	4.86 E+18	6.68 E+18
Projection	2.53E+08	7.57 E+08	24.00	3.59 E+18	5.81 E+18	7.12 E+18	9.62 E+18
Projection	2.53E+08	1.01E+09	32.00	4.75 E+18	7.71 E+18	9.39 E+18	1.26E+19
Projection	2.53E+08	1.26E+09	40.00	5.91 E+18	9.61 E+18	1.17E+19	1.55E+19
Projection	2.53E+08	1.51E+09	48.00	7.07 E+18	1.15E+19	1.39E+19	1.84E+19
Projection	1.89E+08	1.70E+09	54.00	7.94 E+18	1.29E+19	1.56E+19	2.06E+19

Table 6-2 cont'd
Calculated Azimuthal Variation of Fast Neutron Exposure Rates
And Iron Atom Displacement Rates At the Reactor Vessel
Clad/Base Metal Interface

Cycle	Cycle Length [EFPS]	Cumulative Irradiation Time [EFPS]	Cumulative Irradiation Time [EFY]	Iron Atom Displacement Rate [dpa/s]			
				0°	15°	30°	45°
1	3.94E+07	3.94E+07	1.25	1.09E-11	1.71E-11	2.19E-11	3.37E-11
2	3.23E+07	7.16E+07	2.27	9.61E-12	1.36E-11	1.87E-11	2.83E-11
3	3.72E+07	1.09E+08	3.45	7.83E-12	1.26E-11	1.91E-11	2.94E-11
4	3.34E+07	1.42E+08	4.51	8.00E-12	1.21E-11	1.54E-11	2.31E-11
5	4.31E+07	1.85E+08	5.87	7.56E-12	1.13E-11	1.42E-11	1.94E-11
6	4.01E+07	2.25E+08	7.14	7.91E-12	1.23E-11	1.43E-11	1.95E-11
7	4.18E+07	2.67 E+08	8.47	7.63E-12	1.21E-11	1.45E-11	1.92E-11
8	4.04E+07	3.08 E+08	9.75	6.79E-12	1.10E-11	1.33E-11	1.75E-11
9	5.13E+07	3.59 E+08	11.38	7.43E-12	1.12E-11	1.35E-11	1.81E-11
10	4.72E+07	4.06 E+08	12.87	6.63E-12	1.16E-11	1.41E-11	1.77E-11
11	4.58E+07	4.52 E+08	14.27	7.19E-12	1.31E-11	1.53E-11	1.78E-11
Projection	5.29E+07	5.05 E+08	16.00	7.45E-12	1.20E-11	1.44E-11	1.88E-11
Projection	2.53E+08	7.57 E+08	24.00	7.45E-12	1.20E-11	1.44E-11	1.88E-11
Projection	2.53E+08	1.01E+09	32.00	7.45E-12	1.20E-11	1.44E-11	1.88E-11
Projection	2.53E+08	1.26E+09	40.00	7.45E-12	1.20E-11	1.44E-11	1.88E-11
Projection	2.53E+08	1.51E+09	48.00	7.45E-12	1.20E-11	1.44E-11	1.88E-11
Projection	1.89E+08	1.70E+09	54.00	7.45E-12	1.20E-11	1.44E-11	1.88E-11

Table 6-2 cont'd

Calculated Azimuthal Variation of Maximum Exposure Rates

And Integrated Exposures at the Reactor Vessel

Clad/Base Metal Interface

Cycle	Cycle Length [EFPS]	Cumulative Irradiation Time [EFPS]	Cumulative Irradiation Time [EFPY]	Iron Atom Displacements [dpa]			
				0°	15°	30°	45°
1	3.94E+07	3.94E+07	1.25	4.31E-04	6.74E-04	8.60E-04	1.33E-03
2	3.23E+07	7.16E+07	2.27	7.41E-04	1.11E-03	1.46E-03	2.24E-03
3	3.72E+07	1.09E+08	3.45	1.03E-03	1.58E-03	2.17E-03	3.33E-03
4	3.34E+07	1.42E+08	4.51	1.30E-03	1.99E-03	2.69E-03	4.10E-03
5	4.31E+07	1.85E+08	5.87	1.63E-03	2.47E-03	3.30E-03	4.94E-03
6	4.01E+07	2.25E+08	7.14	1.94E-03	2.96E-03	3.87E-03	5.72E-03
7	4.18E+07	2.67 E+08	8.47	2.26E-03	3.47E-03	4.47E-03	6.52E-03
8	4.04E+07	3.08 E+08	9.75	2.53E-03	3.91E-03	5.01E-03	7.22E-03
9	5.13E+07	3.59 E+08	11.38	2.91E-03	4.48E-03	5.70E-03	8.15E-03
10	4.72E+07	4.06 E+08	12.87	3.23E-03	5.03E-03	6.36E-03	8.99E-03
11	4.58E+07	4.52 E+08	14.27	3.56E-03	5.63E-03	7.06E-03	9.80E-03
Projection	5.29E+07	5.05 E+08	16.00	3.95E-03	6.27E-03	7.83E-03	1.08E-02
Projection	2.53E+08	7.57 E+08	24.00	5.83E-03	9.31E-03	1.15E-02	1.55E-02
Projection	2.53E+08	1.01E+09	32.00	7.71E-03	1.23E-02	1.51E-02	2.03E-02
Projection	2.53E+08	1.26E+09	40.00	9.59E-03	1.54E-02	1.88E-02	2.50E-02
Projection	2.53E+08	1.51E+09	48.00	1.15E-02	1.84E-02	2.24E-02	2.98E-02
Projection	1.89E+08	1.70E+09	54.00	1.29E-02	2.07E-02	2.51E-02	3.33E-02

Table 6-3

Relative Radial Distribution Of Neutron Fluence ($E > 1.0$ MeV)

Within The Reactor Vessel Wall

RADIUS (cm)	AZIMUTHAL ANGLE			
	0°	15°	30°	45°
220.35	1.000	1.000	1.000	1.000
225.87	0.545	0.546	0.550	0.540
231.39	0.263	0.263	0.266	0.256
236.90	0.122	0.121	0.123	0.116
242.42	0.056	0.054	0.056	0.050
Note:	Base Metal Inner Radius = 220.35 cm Base Metal 1/4T = 225.87 cm Base Metal 1/2T = 231.39 cm Base Metal 3/4T = 236.90 cm Base Metal Outer Radius = 242.42 cm			

Table 6-4

Relative Radial Distribution of Iron Atom Displacements (dpa)

Within The Reactor Vessel Wall

RADIUS (cm)	AZIMUTHAL ANGLE			
	0°	15°	30°	45°
220.35	1.000	1.000	1.000	1.000
225.87	0.642	0.639	0.648	0.638
231.39	0.396	0.390	0.402	0.338
236.90	0.240	0.235	0.245	0.228
242.42	0.138	0.133	0.139	0.118
Note:	Base Metal Inner Radius = 220.35 cm Base Metal 1/4T = 225.87 cm Base Metal 1/2T = 231.39 cm Base Metal 3/4T = 236.90 cm Base Metal Outer Radius = 242.42 cm			

Table 6-5

Calculated Fast Neutron Exposure of Surveillance Capsules

Withdrawn from Diablo Canyon Unit 1

Capsule	Irradiation Time [EFPY]	Fluence (E > 1.0 MeV) [n/cm ²]	Iron Displacements [dpa]
S	1.25	2.84E+18	4.80E-03
Y	5.87	1.05E+19	1.77E-02
V	14.27	1.37E+19	2.28E-02

Table 6-6

Calculated Surveillance Capsule Lead Factors

Capsule ID And Location	Status	Lead Factor
S (40°)	Withdrawn EOC 1 (for analysis)	3.46
Y (40°)	Withdrawn EOC 5 (for analysis)	3.44
T (40°)	Withdrawn EOC 5 (for storage)	3.44
Z (40°)	Withdrawn EOC 5 (for storage)	3.44
V (4° → 40°)	Withdrawn EOC 11 (for analysis)	2.26
U (4°)	In Reactor	1.28
W (4°)	In Reactor	1.28
X (4°)	In Reactor	1.28
A (4°)	In Reactor	1.31
B (40°)	In Reactor	3.46
C (40°)	In Reactor	3.46
D (40°)	In Reactor	3.46

Notes:

1. Capsule V was irradiated at a 4° location for Cycles 1 through 5, and at a 40° location during Cycles 6 through 11, after which it was removed from service.
2. Lead factors for capsules remaining in the reactor are based on projected exposure calculations through 54 EFPY.
3. Capsules A, B, C, and D were not inserted into position until the beginning of cycle 6.
4. Capsule C is estimated to be withdrawn at the end of cycle 12.

7 SURVEILLANCE CAPSULE REMOVAL SCHEDULE

The following surveillance capsule removal schedule was developed by PG&E and it meets the requirements of ASTM E185-82. This recommended removal schedule is applicable to 32 EFPY of operation.

Capsule	Location	Lead Factor ^(a)	Removal Time (EFPY) ^(b)	Fluence (n/cm ² , E > 1.0 MeV) ^(a)
S	320°	3.46	1.25 (Tested, 1R1)	0.284
Y	40°	3.44	5.86 (Tested, 1R5)	1.05
T	140°	3.44	5.86 (Removed, 1R5)	1.05
Z	220°	3.44	5.86 (Removed, 1R5)	1.05
V	320°	2.26	14.27 (Tested, 1R11)	1.37
C ^(c)	140°	3.46	15.9 (Estimated)	2.31 ^(e)
D ^(c)	220°	3.46	20.7 ^(d) (Estimated)	2.91 ^(e)
B ^(c)	40°	3.46	20.7 (Estimated)	2.91 ^(e)
A ^(c)	184°	1.31	Standby	-
U	356°	1.28	Standby	-
X	176°	1.28	Standby	-
W	4°	1.28	Standby	-

Notes:

- (a) Updated in Capsule V dosimetry analysis [$\times 10^{19}$ n/cm², E > 1.0 MeV], see Table 6-5.
- (b) Effective Full Power Years (EFPY) from plant startup. Beginning with cycle 11, the rated full power changed from 3338 to 3411 MWt.
- (c) Installed at 5.86 EFPY (EOC5).
- (d) Anneal at 15.9 EFPY and reinsert.
- (e) Projected fluence on capsule at proposed withdrawal date. Fluence on capsule equals fluence on the vessel at the given EFPY * Lead Factor.

8 REFERENCES

1. Regulatory Guide 1.99, Revision 2, *Radiation Embrittlement of Reactor Vessel Materials*, U.S. Nuclear Regulatory Commission, May, 1988.
2. Code of Federal Regulations, 10CFR50, Appendix G, *Fracture Toughness Requirements*, and Appendix H, *Reactor Vessel Material Surveillance Program Requirements*, U.S. Nuclear Regulatory Commission, Washington, D.C.
3. WCAP-8465, *Pacific Gas and Electric Co. Diablo Canyon Unit No. 1 Reactor Vessel Radiation Surveillance Program*, J.A. Davidson, et. al., dated January 1975.
4. WCAP-11567, *Analysis of Capsule S from the Pacific Gas and Electric Company Diablo Canyon Unit 1 Reactor Vessel Radiation Surveillance Program*, S.E. Yanichko, et. al., dated December 1987.
5. WCAP-13750, *Analysis of Capsule Y from the Pacific Gas and Electric Company Diablo Canyon Unit 1 Reactor Vessel Radiation Surveillance Program*, E. Terek, et. al., dated July 1993.
6. ASTM E185-82, *Standard Practice for Conducting Surveillance Tests for Light-Water Cooled Nuclear Power Reactor Vessels*.
7. ASTM E23-98, *Standard Test Method for Notched Bar Impact Testing of Metallic Materials*, ASTM, 1998.
8. ASTM A370-97a, *Standard Test Methods and Definitions for Mechanical Testing of Steel Products*, ASTM, 1997.
9. ASTM E8-99, *Standard Test Methods for Tension Testing of Metallic Materials*, ASTM, 1999.
10. ASTM E21-92 (1998), *Standard Test Methods for Elevated Temperature Tension Tests of Metallic Materials*, ASTM, 1998.
11. Procedure RMF 8402, *Surveillance Capsule Testing Program*, Revision 2.
12. Procedure RMF 8102, *Tensile Testing*, Revision 1.
13. Procedure RMF 8103, *Charpy Impact Testing*, Revision 1.
14. WCAP-14370, *Use of the Hyperbolic Tangent Function for Fitting Transition Temperature Toughness Data*, T. R. Mager, et al, May 1995.
15. ASTM E208, *Standard Test Method for Conducting Drop-Weight Test to Determine Nil-Ductility Transition Temperature of Ferritic Steels*, in ASTM Standards, Section 3, American Society for Testing and Materials, Philadelphia, PA.

16. Section XI of the ASME Boiler and Pressure Vessel Code, Appendix G, *Fracture Toughness Criteria for Protection Against Failure*.
17. ASTM E185-70, *Recommended Practice for Surveillance Tests for Nuclear Reactor Vessels*.
18. ASTM E83-93, *Standard Practice for Verification and Classification of Extensometers*, in ASTM Standards, Section 3, American Society for Testing and Materials, Philadelphia, PA, 1993.
19. Regulatory Guide RG-1.190, *Calculational and Dosimetry Methods for Determining Pressure Vessel Neutron Fluence*, U. S. Nuclear Regulatory Commission, Office of Nuclear Regulatory Research, March 2001.
20. WCAP-14040-NP-A, Revision 2, *Methodology Used to Develop Cold Overpressure Mitigating System Setpoints and RCS Heatup and Cooldown Limit Curves*, January 1996.
21. WCAP-15557, Revision 0, *Qualification of the Westinghouse Pressure Vessel Neutron Fluence Evaluation Methodology*, August 2000.
22. RSICC Computer Code Collection CCC-650, *DOORS 3.1, One, Two- and Three-Dimensional Discrete Ordinates Neutron/Photon Transport Code System*, August 1996.
23. RSIC Data Library Collection DLC-185, *BUGLE-96, Coupled 47 Neutron, 20 Gamma-Ray Group Cross Section Library Derived from ENDF/B-VI for LWR Shielding and Pressure Vessel Dosimetry Applications*, March 1996.
24. WCAP-15780, *Fast Neutron Fluence and Neutron Dosimetry Evaluations for the Diablo Canyon Unit 1 Reactor Pressure Vessel*. December 2001.
25. PG&E Letter No. DCL-92-072, *Diablo Canyon Unit 1 Supplemental Reactor Vessel Radiation Surveillance Program*, March 1992.
26. WCAP-13440, Revision 0, *Supplemental Reactor Vessel Radiation Surveillance Program for the Pacific Gas and Electric Company Diablo Canyon Unit No. 1*, December 1992.
27. Combustion Engineering Report CE NPSD-1039, Revision 2, *Best Estimate Copper and Nickel Values in CE Fabricated Reactor Vessel Welds*, June 1997.